KWAME NKRUMAH UNIVERSITY OF SCIENCE AND TECHNOLOGY, KUMASI, GHANA

COLLEGE OF ENGINEERING
FACULTY OF CIVIL AND GEOMATIC ENGINEERING

APPLICATION OF TOPKAPI MODEL FOR RUNOFF ESTIMATION AND LANDUSE MANAGEMENT AT PUNGU NEAR NAVRONGO

KNUST

A Thesis submitted to the Board of Graduate Studies, Kwame Nkrumah University of Science and Technology, in fulfilment of the requirement for the Award of the Degree of Master of Philosophy in Water Resources Engineering and Management
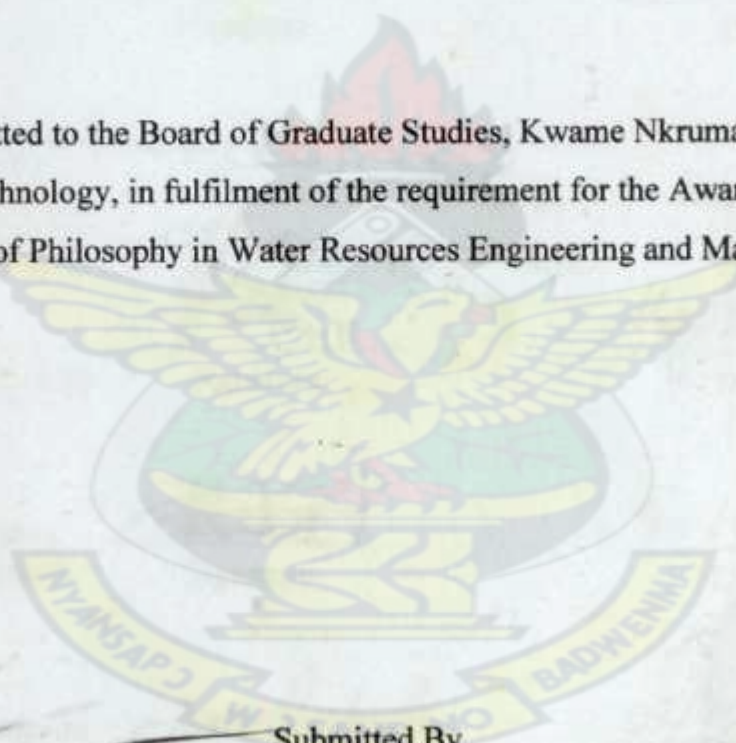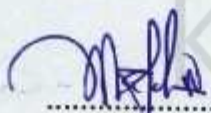
Submitted By
Mawuli Lumor
BSc. Physics (Hons)

February 2009

CERTIFICATION

I hereby declare that this submission is my own work towards the Master of Philosophy and that, to the best of my knowledge, it contains no material previously published by another person nor material which has been accepted for the award of any other degree of the University, except where due acknowledgement has been made in the text

Lumor Mawuli 30/04/09
Signature Date

Certified by:

Dr. S. N. Odai .... May 8 2009
(Principal Supervisor) Signature Date

Mr. K. A. Amaning 30/04/09
(Second Supervisor) Signature Date

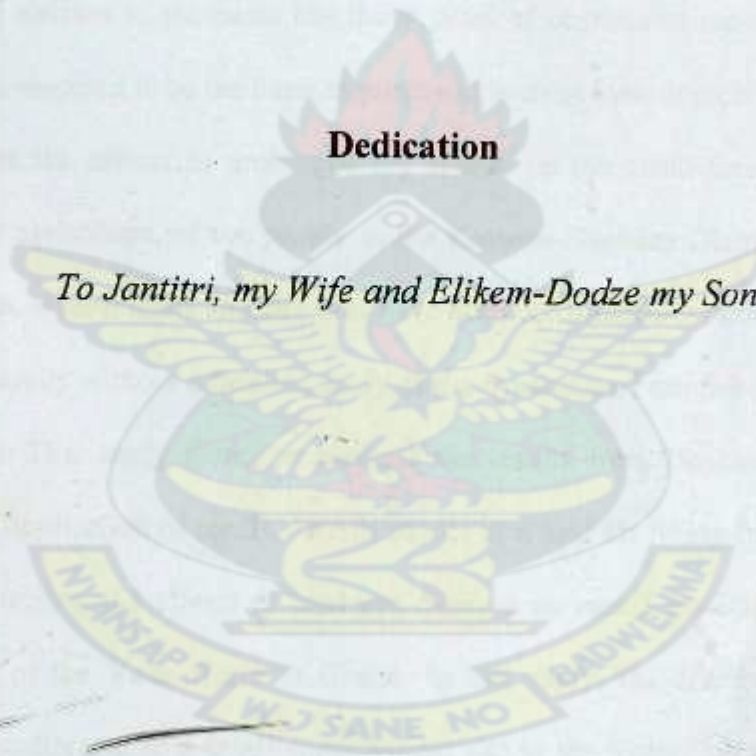Prof. S. I. K. Ampadu 09/05/2009
(Head of Department) Signature Date

Dedication

To Jantitri, my Wife and Elikem-Dodze my Son.

iii

Abstract

The Hydrological Services Department of the Ministry of Water Resources Works and Housing in Ghana is the body mandated to collect, analyse, store and disseminate runoff data on all river networks through the development of hydrological monitoring networks in the country. However, the number of hydrological monitoring networks established in the Volta Basin in Ghana has declined by 48% over the years due to lack of adequate resources to operate and maintain them. Furthermore, only 38% of the networks which are currently still in operation have stage-discharge measurements which are necessary for the generation of runoff data. Significantly, none of the monitoring stations in the basin has thirty years of continuous runoff data which is generally considered to be the basic requirement in most hydrological analysis. Again, to minimize the effects of prolonged dry season on the socio-economic activities, subsistence agriculture, of the people in the Kassena-Nankana District of the Upper East Region, several dams and dug-outs have been constructed to address the problem of water scarcity without a detailed study of the dynamics of rainfall-runoff processes in the area. This study therefore presents the results from field observations and subsequent application of the TOPKAPI model as a tool for filling-in missing runoff data and studying the effects of land use changes on runoff generation in the sub-catchments of the Volta Basin in Ghana. In this study, the distributed TOPKAPI model was calibrated in a small experimental site in the Volta Basin at Pungu near Navrongo in the Kasena-Nakana District of the Upper East Region. The model was calibrated using field observations as input data. The calibrated model was used as a tool to fill-in missing runoff data in the Nabogo catchment, a sub-catchment of the Volta Basin. The model was also used to test different scenarios of land-use changes. With a model efficiency of 0.877, the TOPKAPI model provided reasonable estimates

of missing runoff data in the Nabogo catchment in the Volta Basin. Results from the quantitative assessment of the land-use scenarios also show that tillage conservation increases water movement into the soil leading to high percentage of saturation volumes and subsequently declining mean annual runoff. Finally, the model was found to be more sensitive to the channel Manning's roughness coefficient than that of the surface Manning's roughness coefficient.

Table of Contents

List of Figures

viii

KNUST

viii

KNUST

List of Tables

List of Plates

List of Abbreviations

Ce	Coefficient of Efficiency
CV	Coefficient of Variation
DEM	Digital Elevation Model
DGPS	Differential Global Position System
DSS	Decision Support System
GCAG	Ghana – Country at a Glance
GCMs	Global Circulation Models
GIS	Geographic Information System
ILWIS	Integrated Land and Water Information System
Ks	Hydraulic Conductivity
n_c	Channel Manning's roughness coefficient
n_s	Surface Manning's roughness coefficient
S	Simple Sensitivity Index
SHE	Système Hydrologique Européen
TIN	Triangular Irrigular Network
TOPKAPI	TOPographic Kinematic Approximation and Integration
UH	Unit Hydrograph
USDA	United States Department of Agriculture
WGS	World Geodetic System

Acknowledgements

I am most grateful to God Almighty for his grace and mercy and for seeing me through this study. I am indeed indebted to Prof. E. Allotey and the Glowa-Volta Project for accepting to sponsor my study. I am highly indebted to Dr. S. N. Odai for the technical advice and invaluable support he gave through out the research. You did not only supervise my work but you held my hand and lifted me up when I was down. I am most grateful.

Special thanks go to Mr. Kwaku A. Amaning, my second supervisor for his constructive advice and suggestions. I would like to express my sincere and heartfelt appreciation to Mr. Frank O. Annor for his support and assistance during the course of this work.

I am grateful to all the lecturers in the Civil Engineering Department for their constructive advice, comments and suggestions. My appreciation goes to Mr. Wise V. Ametepe of the Hydrological Service Department for being with me throughout the course of this work.

Finally, I thank my family especially my Mom, Madam Hilda F. Adda, for their support and encouragement.

1 INTRODUCTION

1.1 Background

Human induced global climate and land use changes directly affect runoff, vegetation structure and plant productivity. However, spatial and temporal patterns of changes may differ in different regions, like the patterns of temperature and precipitation derived from simulation runs performed with global circulation models (GCMs).

Surface runoff is a term used to describe the flow of water from rain, snowmelt or other sources over the land surface, and is a major component of the water cycle. Surface runoff (flux at a point in space), often used interchangeably with the term overland flow (a spatially distributed phenomenon), resulting from precipitation-runoff transformation process plays a significant part in the hydrological cycle (Ajayi et al, 2004).

Significantly, substantial progress has been made in understanding the hydrologic process of rainfall-runoff process and its impact on the global water cycle in some parts of the world. However, very little has been done in sub-Saharan Africa countries (van de Giesen et al., 2000), particularly in West Africa. Only few examples exist of detailed hydrological studies that use sub-daily information on small experimental catchments (Chevallier and Planch, 1993).

1

Overland flow significantly influences the amount of water available in rivers, streams and ponds, and determines the size and shape of flood peaks (Troch et al., 1994). Surface runoff, when properly managed through runoff harvesting, could be converted into valuable water resources for agricultural production in floodplain farming. This could be very useful in most sub-Saharan African countries, facing a consistent trend of declining or fluctuating annual rainfall totals, which is affecting food production under rain-fed agriculture (FAO, 1995).

According to Opoku-Ankomah (2000), in recent years, there have been a number of changes in the precipitation patterns of some sub-catchments in the Volta Basin, as rainfall and run-off reductions have been evident since the 1970s. Some areas that used to have bi-modal type of rainfall now have uni-modal type as the second minor season has become very weak or non-existent. This situation means that rain-fed agriculture can only be carried out once instead of twice a year. Studies in the basin have indicated that 340 km^3 of rain must fall on the catchment before run-off occurs at significant level. Once this threshold has been reached, approximately half of the precipitation becomes run-off. This indicates that only small changes in rainfall could have dramatic effects on run-off rates. Although rainfall decreased by only 5% from 1936 to 1998, run-off decreased by 14% (Andreini, 2000).

Located in the Guinea Savannah belt, the Kassena-Nankana District's ecology is typically Sahelian (hot and dry), with the vegetation consisting mostly of semi-arid grassland interspersed with short trees. There are two main climatic seasons, the wet and dry seasons. The wet season extends from April to October, with the heaviest rainfall mainly occurring between June and October. The mean annual rainfall is 900

2

mm but the highest level is recorded in August. Similarly, the dry season is subdivided into the Harmattan (November to mid February) and the dry hot (mid February to April) seasons. Monthly temperatures range from 20°C to 40°C, with the minimum and maximum temperatures occurring in December and March respectively.

Subsistence agriculture is the mainstay of the district's economy. About 90% of the people are farmers. The major agricultural products are groundnuts, millet, guinea corn, rice, sorghum, sweet potatoes, beans and tomatoes. Unfortunately, the rainfall pattern limits food cultivation to a single growing season. Weather conditions in the area can be very severe, resulting in either occasional floods or droughts and, therefore, poor harvests. This situation has culminated in the net annual out-migration of the population for some time now (Binka et al, 1999).

In order to minimize the effects of prolonged dry season on the socio-economic activities of the people and roll out interventions, there is the need to understand the dynamics of rainfall-runoff processes in the area. The need for stream flow statistics for designing structures such as reservoirs, developing environmentally sound river basin management plans, siting and permitting of new water withdrawals, interbasin transfers, discharges of pollutants, determining the stream flow needs of aquatic plants and animals, land-use planning and the design and management of water supplies systems cannot be over emphasized. Unfortunately, however, country reports of the United Nations Development Programme (UNDP)/World Bank indicate that the hydrological monitoring networks in Sub-Saharan Africa have declined substantially (WMO-WHYCOS, 2005).

The Hydrological Services Department of the Ministry of Water Resources, Works and Housing is the body mandated to carry-out hydrological surveys in Ghana. This involves among others, the collection, analysis, storage and dissemination of runoff on all river networks in the country. The department, in line with its mandate, has established 124 hydrological monitoring stations in the Volta Basin since its establishment. Over the years, the numbers of these hydrological monitoring stations in the basin have declined by 48%. Unfortunately, only 38% of the operating hydrological stations have stage-discharge measurement and none of the hydrological stations has 30 years of continuous data which is generally considered as a basic requirement for hydrological and water resources management analysis.

Furthermore, due to dwindling resources, only the major rivers in the basin are currently being monitored with consequent neglect of the minor streams. Hence, the need for a reliable hydrological model that can best simulate the runoff regimes in the basin is long overdue. The need to understand the effects of changing land-use on runoff in the basin also requires a comprehensive and reliable hydrological model that can best represent the hydrologic process at the local scale.

In this study the TOPKAPI model, a distributed rainfall-runoff hydrologic model, was calibrated, validated and applied in a small catchment at Pungu near Navrongo in the Kassena-Nankana District of the Upper East Region. Furthermore, different "what ifs" scenarios were tested on the impact of land-use change on runoff generation within the catchment using the model.

4

1.2 Research Goals and Objectives

Within the context of the GLOWA Volta Project, which was setup to develop a decision support system (DSS), for sustainable water management in the Volta Basin, a comprehensive monitoring and simulation framework that will assist decision makers to evaluate the impact of manageable (irrigation, primary water use, land-use change, power generation, trans-boundary water allocation) and less manageable (climate change, rainfall variability, population pressure) factors on the social, economic, and biological productivity of water resources is provided. The objectives of this study are to:

1. Calibrate and validate the distributed TOPKAPI model in a small experimental site within the White Volta Basin at Pungu in the Kassena-Nankana District of the Upper East Region.

2. Use the calibrated model as a tool for data in-filling in hydrological monitoring stations with long periods of missing data in the Volta Basin.

3. Study the effects of the land-use change on surface runoff processes in the experimental site.

1.3 Justification

Surface runoff or overland flow is often recognized as one of the key components of the hydrological process. However, it has hardly been studied in detail at the local level in the White Volta Basin. Consequently, a knowledge gap still exists concerning the hydrologic behavior of the catchment in spite of the importance of the basin to Ghana in terms of hydro-power generation, irrigation, river navigation and water supply. There is therefore a general need for an efficient and effective hydrological model which can simulate the runoff process in the basin.

5

The ultimate scientific challenge is: can the hydrograph of the study area be predicted using information on topography, land-use, geomorphology, and soil data? In other words, what possibilities exist for the distributed TOPKAPI model to be used as a reliable tool that can be employed to fill-in-gaps for hydrological monitoring stations where there is missing data or predict runoff data for ungauged tributaries within the White Volta Basin where no data exist by considering the various components of the hydrologic process while assessing the hydrological consequences of land use change in the basin? This is challenging but achievable.

2 LITERATURE REVIEW

2.1 Review of Hydrological Models

A management change imposed on one component of the environmental continuum has effects that propagate to other components, and some of these effects are unknown and cannot be quantified. Integrated water management can therefore be accomplished within a spatial unit called watershed through the instrument of modeling (Singh, 1995).

Hydrologic modeling inevitably requires simplification or abstraction. Indeed, it has been found through experience that understanding and predicting the behavior of any significant part of the environment requires abstraction. Abstraction consists in replacing the part of the universe under consideration by a model of simpler structure. Models, formal or intellectual on the one hand or material on the other, are thus a central necessity of scientific procedure (Rosenbleuth and Wiener, 1945).

Hydrologic models are approaches which represent mathematically both the individual process and all the interrelated processes involved in the hydrologic cycle, by means of a group of balance equations, which express the balance in terms both of mass and of momentum and/or energy, while the interactions between the various processes must be represented by matching the boundary conditions of the various systems of differential equations.

7

Models may be empirical, deterministic, or stochastic. Ward et al, (1995) define the various forms of models as follows: Empirically-based models are developed by analyzing a large set of data, and developing statistical relationships between inputs and outputs; Deterministic models, sometimes described as theoretical or process-based models, mathematically describe the processes being modelled, such as runoff. As the processes are independent of geographic variations, deterministic models can be applied to a wider range of conditions than empirical; Stochastic models seek to identify statistical probabilities of hydrologic events, like rainfall or flood flows, and to predict the probability of a given outcome. The stochastic models also consider the natural variability that might occur in some model input parameters.

2.1.1 The Rational and the Time-Area Methods

There are many empirical rainfall-runoff models of similar form that require input of rainfall estimates for storms of given frequencies. Possibly the best known is the simple and aptly named Rational formula (Linsley et al., 1949). The rational method is usually attributed to Kuichling (1989) and Lloyd-Davies (1906), but Mulvaney (1851) clearly outlined the procedure in a paper in Ireland. The Rational equation is the simplest of the available methods, and has spawned numerous ways of computing the coefficient "C" and the time of concentration (Ward et al., 1995).

The equation is rational and useful as long as the rainfall intensity is for duration equal to the time of concentration and the area is small enough to ensure relatively homogeneous rainfall and watershed characteristics. Analyses suggested that, although the method can result in large errors in any given case, it may, on the average, give reasonable design results (Shaake et al., 1967).

8

The rational method has been extended to include non-uniform rainfall and irregular areas through the use of time-area methods, which involve a time-area curve indicating the distribution of travel times from different parts of the basin (Bedient and Huber, 1992). The approach does not consider interflow and assumes that surface and channel flow velocities do not change with time.

2.1.2 The Unit Hydrograph

One approach to developing a storm runoff hydrograph is the unit hydrograph method. Sherman (1932) originally advanced the theory of the unit hydrograph (UH), defined as "basin outflow resulting from one inch (1 cm) of direct runoff generated uniformly over the drainage area at a uniform rainfall rate during a specified period of rainfall duration." It is the most venerable and widely used transfer function for systems modeling of hydrologic response (Dingman, 1994).

Several assumptions inherent in the unit hydrograph tend to limit its application (Johnstone and Cross, 1994) for a given watershed:

i.   Rainfall excesses of equal duration are assumed to produce hydrographs with equivalent time bases regardless of the intensity of the rain.

ii.   Direct runoff ordinates for a storm of given duration assumed directly proportional to rainfall excess volumes. Thus, twice the rainfall produces a doubling of hydrograph ordinates.

iii. The time distribution of direct runoff is assumed independent of antecedent precipitation.

iv.   Rainfall distribution is assumed to be the same for all storms of equal duration, spatially and temporally.

9

The classic statement of unit hydrograph theory can be summarized briefly: the hydrologic system is linear and time-invariant (Dooge, 1973). The property of proportionality and the principle of superposition both apply to the unit hydrograph but were not seriously questioned until the mid- 1950's. While the assumptions of linearity and time invariance are not strictly correct for a watershed, they are adopted as long as they are useful.

The basic factors which need to be determined in order to develop a unit hydrograph are; the time to peak, the peak flow and the shape of the hydrograph. In practice, the unit hydrograph is used to predict or forecast watershed response to a specified water input event.

2.1.3 The Linear Models

The unit hydrograph concept was found to be responsive to a causative, linear, dynamic, time invariant system and the use of mathematical techniques such as Z, Laplace or Fourier transforms could lead to the derivation of the response function from the analysis of the system's input and output data.

Nash (1958) advanced the conceptual model of a watershed as a cascade of n reservoirs in series, each with a linear storage-discharge relation. Dooge (1959) produced a general conceptual model of the unit hydrograph. Since the unit hydrograph existed for a linear system, linear storage elements and linear distortionless channels should be components of the model. Both translation effects and storage or attenuation effects exist in an actual watershed. It was assumed that

10

since the model is linear, the translation effects were lumped together as linear channels and the storage effects were lumped together as linear reservoirs. Because of linear superposition, channels and reservoirs could be interchanged or reordered without affecting the response of the system. Diskin and Simon (1979) simplified the Dooge linear model by modeling the watershed response with two cascades of equal linear reservoirs in parallel.

2.1.4 Conceptual Models

Conceptual rainfall-runoff models are widely used tools in hydrology. Contrary to more complex, physically-based, distributed models such as the SHE model (Abbott et al, 1986a), the required input data are readily available for most applications. Furthermore, conceptual models are usually simple and relatively easy to use. In spite of the attractiveness of conceptual models, they suffer from some fundamental problems. One such problem is that conceptual models often are over-parameterized with intercorrelated model parameters (Jakeman & Hornberger, 1993; Gaume et al, 1998). Some model parameters have a physical basis, but since they are effective parameters on the catchment scale, they are hardly measurable in the field. This makes the calibration of a conceptual model inevitable. However, it is often not possible to find one unique "best" parameter set, i.e. different parameter sets give similar good results during a calibration period (Mein & Brown, 1978). Parameter uncertainty also makes simulations for periods outside the calibration period less reliable (Harlin & Kung, 1992). In addition, "model uncertainty" may exist, i.e. an uncertainty about which model to choose (Melching et al., 1990). During model development, concepts of catchment hydrology are implemented into the model as a simplified representation of real processes. The user has to decide which one of the

11

many existing models is suitable and choose the spatial delineation such as, for instance, the number of elevation or land-use zones. Usually, for most of these decisions there is a lack of objective criteria (Mroczkowski et al., 1997).

2.1.5 Distributed Models

The response of natural catchments to precipitation depends on the mechanisms of runoff generation and their spatial and temporal distribution (Vivoni et al, 2007). Nevertheless, quantitative descriptions of distributed runoff generation are difficult to acquire in field settings. To address this, a number of distributed hydrologic models, such as the TOPMODEL (Beven and Kirkby, 1979), the Système Hydrologique Européen (SHE) Model (Abbot et al., 1986b) and the TOPKAPI (Todini, 1995), have been developed to represent multiple runoff mechanisms and their variability in a catchment (Smith and Hebbert, 1983).

Given their capability of representing the internal spatial hydrological pattern, the major areas of application of distributed models can be found in forecasting the effects of land-use change, the effects of spatially variable inputs and outputs, the movement of pollutants and sediments, and the hydrologic response of ungauged catchments (Beven and O'Connell, 1982).

Watersheds may be modeled by a lumped model using basin average input data and producing total basin stream flow. Such a model may produce reasonable results but because of the distributed nature of hydrological properties like soil type, slope and land-use, the model cannot be expected to accurately represent the watershed conditions. For connection of topography, the computer-based methodology known as

12

Geographic Information System (GIS) is quite good to cover the link between the topographic, land-use and other information related to geographical location. It is applied to a hydrologic system to assess the impact due to land-use change. Remote sensing technique because of its capability of synoptic viewing and repetitive coverage provides useful information on land-use dynamics. With the development of GIS, the hydrological catchment models have been more physically based and distributed considering spatial heterogeneity.

2.2 Review of other Distributed Hydrologic Models

In this section, analysis of two well known and widely used semi-distributed hydrological models, namely the ARNO and the TOPMODEL are presented against the backdrop of a detailed description of the physically-based distributed TOPKAPI model used for this study.

2.2.1 The ARNO Model

The ARNO model (Todini, 1996), following the earlier work of Zhao (1977), is a variable contributing area semi-distributed conceptual model driven by the total soil moisture storage, which is functionally related, by means of simple analytical expressions, to the directly contributing areas, the evapo-transpiration, the drainage and the percolation. This makes the model extremely useful in evaluating the total amount of soil moisture available for evapo-transpiration, which is one of the major requirements for inclusion in Global Circulation Models, GCMs (Todini and Dümenil, 1999).

The major disadvantage of the ARNO model in this respect is the lack of physical grounds for establishing some of the parameters, and in particular those relevant to the "drainage" namely the horizontal movement in the unsaturated zone, which have to be estimated on the basis of the available precipitation and runoff data; this is not particularly critical in hydrological applications but it becomes so when the model is used in GCMs, where direct input/output observations are not really available (Todini and Dümenil, 1999).

2.2.2 The TOPMODEL

The TOPMODEL (Beven and Kirkby, 1979) is a variable contributing area lumped conceptual model in which the predominant factors determining the formation of run-off are represented by the topography of the basin and a negative exponential law linking the transmissivity of the soil with the distance of the saturated zone below ground surface. The TOPMODEL is attractive in that it can be considered as a "simple physically-based conceptual model" (Sivapalan et al., 1987), in the sense that its parameters can be measured directly, or more realistically in the sense that its parameters can be physically interpreted. Despite the caution in accepting the definition of physically-based model, the inclusion of the effects of variability of topography on contributing area dynamics represents a major advance over previous models based on "point" hydrological responses assumed to apply at the catchment scale. The TOPMODEL represents a first attempt to combine the computational and parametric efficiency of a lumped approach with the link to physical theory and possibilities for more rigorous evaluation offered by a distributed model (Beven et al., 1995).

14

The major disadvantage of TOPMODEL lies in the steady state assumption at a point, which is advocated in order to derive the model integral equation. This assumption becomes unrealistic for cells of the order of magnitude of hundreds of meters, which implies the need for parameter values far beyond their physical limits (Franchini et al., 1996).

From the above analysis, the TOPKAPI, the new rainfall-runoff model, which is used in this study exploits the potential of distributed models based upon physically meaningful parameters (Beven, 1989); to overcome the scale dependency of parameters as in TOPMODEL (Franchini et al., 1996); allowing for, as a consequence of the previous points, the application of the model at increasing spatial scale, from hillslope to catchment scales and, in perspective, to the GCMs (Todini and Dümenil, 1999).

2.2.3 The TOPKAPI Model

TOPKAPI (**TOP**ographic **K**inematic **AP**proximation and **I**ntegration) (Todini and Ciarapica, 2001) is a physically based rainfall-runoff model applicable at different spatial scales, ranging from the hillslope to catchment, and in the perspective to the GCMs scale, maintaining at increasing scales physically meaningful values for the model parameters. The parameterisation is relatively simple and parsimonious.

The TOPKAPI model combines the kinematic approach with a Digital Elevation Model (DEM) describing a basin. Three 'structurally-similar' non-linear reservoirs characterise the model which describes different hydrological and hydraulic processes. The TOPKAPI approach is a comprehensive distributed-lumped approach.

15

The distributed TOPKAPI model is used to identify the mechanism governing the dynamics of the saturated area contributing to the surface runoff as a function of the total water storage, thus obtaining a law underpinning the development of the lumped model. Theoretically it proves the lumped version of the TOPKAPI model can be derived directly from the distributed version without the need for additional calibration.

2.2.3.1 Structure and Methodology of the TOPKAPI Model

The TOPKAPI model is based on the idea of combining the kinematic approach with the topography of the basin; the latter is described by a Digital Elevation Model (DEM), which subdivide the application domain by means of a grid of square cells, whose size generally increases with the overall dimensions, due to the constraints imposed by the computing resources; consequently, increasing the application scale of the model implies an increase in the dimensions of the cells, which at catchment scale may amount to several hundred metres per side. Each cell of the DEM is assigned a value for each of the physical characteristics represented in the model. The flow paths and slopes are evaluated starting from the DEM, according to a neighbourhood relationship based on the principle of the minimum energy cost, namely the maximum elevation difference; it takes account of the links between the active cell and the four surrounding cells connected along the edges, due to the finite difference approach underpinning the model; the active cell is assumed to be connected downstream with a sole cell, while it can receive upstream contributions from more than one cell, up to a maximum of three cells (Band, 1986).

16

The integration in space of the non-linear kinematic wave equations results in three 'structurally-similar' zero-dimensional non-linear reservoir equations. The first represents the drainage in the soil, the second represents the overland flow on saturated or impervious soils and the third represents the channel flow. The parameter values of the model are shown to be scale independent and obtainable from digital elevation maps, soil maps and vegetation or land use maps in terms of slopes, soil permeability's, topology and surface roughness.

The integration of the fundamental equations is performed on the individual cell of the DEM in the distributed model, while in the lumped model it is performed on the basin or sub-basin as a whole, in this way arriving at a problem unconstrained by spatial dimensions. The equations obtained for the local scale and for the lumped scale are structurally similar; what distinguishes them are the coefficients, which in one case have local significance and, in the other, summarise the local properties in a global manner.

The TOPKAPI model is structured around three basic modules which represent the soil water component, the surface water component and the channel water component (drainage network component) respectively (see Figure 2-1). Due to the need to introduce into the model only an essential number of components, for the sake of simplicity, the TOPKAPI model does not account for water percolation towards the deeper soil layers and for their contribution to the discharge.

17
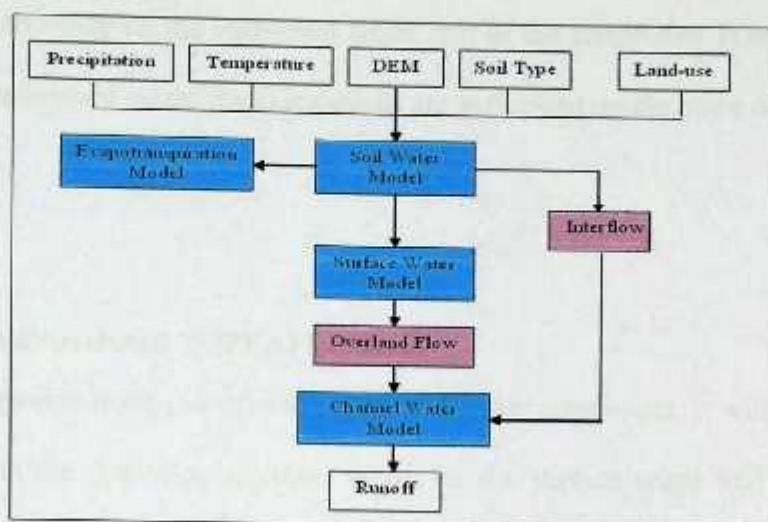
Figure 2-1: A flow structure representing the TOPKAPI Model

The soil water component is affected by a flow of water (interflow or subsurface flow) in a horizontal direction in conditions of non-saturation, defined as drainage; drainage occurs in a surface soil layer, of limited thickness and with high hydraulic conductivity due to its macro-porosity. The drainage mechanism plays a fundamental role in the model both as a direct contribution to the flow in the drainage network, and most of all as a factor regulating the soil's water balance, particularly with regard to activating the production of overland flow. The soil water component is the most characterizing aspect of the model because it regulates the functioning of the contributing saturated areas. The surface water component is activated on the basis of this mechanism. Lastly, both components contribute to feed the drainage network.

The evapotranspiration is taken into account as water loss, subtracted from the soil's water balance. This loss may be a known quantity, if available, or it may be calculated using the temperature data and other topographic, geographic and climatic information. In this case the same method used to calculate evapotranspiration in the ARNO model (Todini, 1996) is adopted. The five components (Figure 2-1) mentioned

18

above are activated on the individual DEM grid in the distributed TOPKAPI model, while in the lumped model the calculations are performed on the basin or sub-basin as a whole.

2.2.4 The Distributed TOPKAPI Model

Given the predominant role played by the soil water component, it will be described in details in the following sections, while for the surface water and the drainage network components, formally having the same structure, only the outstanding features and the final equations will be pointed out.

2.2.4.1 The soil water component

2.2.4.1.1 Basic assumptions:

Precipitation is assumed to be constant over the integration domain (namely the single cell), by means of suitable averaging and lumping operations of the local rainfall data, such as Thiessen polygons techniques, Block Kriging (de Marsily, 1986; Matheron, 1970).

All of the precipitation falling on the soil infiltrates into it, unless the soil is already saturated in a particular zone; this is equivalent to adopting as the sole mechanism for the formation of overland flow the saturation mechanism from below, also known as saturation excess or Dunne mechanism (Dunne,1978), ignoring on the other hand the possible activation of the Hortonian mechanism due to infiltration excess; this decision is justified by the fact that the infiltration excess mechanism is characteristic by a local modeling scale, whereas the saturation excess mechanism, being linked to a

cumulative phenomenon and conditioned by a lateral redistribution movement of the water in the soil, becomes dominant as the scale of the modeling increases (Blöschl and Sivapalan, 1995).

The slope of the water table is assumed to coincide with the slope of the ground, unless the latter is very small (less than 0.01%); this constitutes the fundamental assumption of the approximation of the kinematic wave in the De Saint Venant equations, and it implies the adoption of a kinematic wave propagation model with regard to horizontal flow, or drainage, in the unsaturated area (Henderson and Wooding, 1964; Beven, 1981, 1982; Borah et al., 1980; Sloan and Moore, 1984; Hurley and Pantelis, 1985; Stagnitti et al., 1986; Steenhuis et al., 1988). Local transmissivity, like local horizontal flow, depends on the total water content of the soil, i.e. it depends on the integral of the water content profile in a vertical direction.

Saturated hydraulic conductivity is constant with depth in a surface soil layer but much larger than that of deeper layers; this forms the basis for the vertical aggregation of the transmissivity, and therefore of the horizontal flow, as will be described in details in the following section;

2.2.4.1.2 The vertical lumping

The horizontal flow in unsaturated conditions could be described based on the knowledge of the vertical moisture content profile into the soil. Due to the high conductivity value, caused by macropores in the top of the soil (Beven and Germann, 1982), gravity will be the dominant mechanism driving water from the top of the soil to the bottom (impermeable or semi-impermeable lower boundary). The latter

20

boundary will create a perched water table. In this zone a non-negligible horizontal propagation (also involving unsaturated flow), will occur (Todini, 1995).

Nevertheless, the depth of this high conductive soil (no more than one or two metres) will be negligible with respect to the horizontal grid dimensions. For this reason we can assume that the transient phase of vertical infiltration can be neglected; in other words, when interested in the horizontal movement of water, it is possible to avoid, within the range of reasonable errors, the integration of the unsaturated soil vertical infiltration equation, namely Richards equation (Todini, 1995). The hypotheses 4) and 5) introduced in the previous section play their role in this context, thus representing the basis for vertical lumping of the transmissivity. In practice it is assumed that the horizontal flux evaluated starting from the integration of the vertical soil moisture content profile does not differ strongly from that evaluated assuming the saturated hydraulic conductivity as constant with depth, and introducing the total soil moisture content integrated along the vertical profile (Benning, 1994).

The transmissivity of a soil layer in non-saturated condition is given by the following expression:

$$T = \int_0^L k\left(\tilde{\vartheta}(z)\right)dz$$

(2.1)

where L is the thickness of the layer affected by the horizontal flow; z is the vertical direction; $k\left(\tilde{\vartheta}(z)\right)$ is the hydraulic conductivity in non-saturated condition, a function of the saturation degree; $\tilde{\vartheta} = \dfrac{\vartheta - \vartheta_r}{\vartheta_s - \vartheta_r}$ is the reduced water content; ϑ_r is the residual

21

water content, i.e. water which cannot be removed by capillarity or gravity; ϑ_s is the saturated water content; ϑ is the water content in the soil.

In keeping with the previous hypotheses the transmissivity given by Equation (2.1) is replaced by the following approximated expression:

$$T(\widetilde{\Theta}) = k_s L \widetilde{\Theta}^{\alpha}$$

(2.2)

where k_s is the saturated hydraulic conductivity; $\widetilde{\Theta} = \dfrac{1}{L}\displaystyle\int_0^L \widetilde{\vartheta}(z)dz$ is the mean value along the vertical profile of the reduced water content and α is a parameter dependent on the characteristics of the soil (Benning, 1994; Todini, 1995).

The horizontal flux can therefore be calculated starting from the actual profile, by means of the Brooks and Corey's formula, (Brooks and Corey, 1964),

$$k(\widetilde{\vartheta}) = k_s \widetilde{\vartheta}^{a}$$

$$q = \int_0^L \tan(\beta) k_s \widetilde{\vartheta}^{a} dz$$

(2.3)

The subsurface flow is then calculated for each value of $\widetilde{\Theta}$ by means of the approximated formula (2.4):

$$q = \tan(\beta) k_s L \widetilde{\Theta}^{\alpha}$$

(2.4)

22

2.2.4.1.3 Kinematic wave formulation for sub-surface flow.

The analysis of a generic hydraulic system is usually addressed using the continuity equation and the dynamic equation. In the TOPKAPI model, the dynamic equation is represented by an approximate form expressed by Equation (2.4). Adding the flow equation (2.4), to the continuity of mass equation, one obtains the following system:

$$\begin{cases} (\vartheta_s - \vartheta_r)L \dfrac{\partial \tilde{\Theta}}{\partial t} + \dfrac{\partial q}{\partial x} = p \\ q = \tan(\beta)k_s L \tilde{\Theta}^{\alpha} \end{cases}$$

(2.5)

where x in meters is the main direction of flow along a cell (dimension of the cell), t is the time in seconds, q is the flow in the soil due to drainage, corresponding to a discharge (m³/s) per unit of width (m), and p is the intensity of precipitation in millimeters. The model is written in just one direction since it is assumed that the flow along the slopes is characterized by a preferential direction, which can be described as the direction of maximum slope.

From the combination of the two equations (2.5), rewriting the problem in terms of actual total water content in the soil, along the vertical profile, and substituting the following equations:

$$\eta = (\vartheta_s - \vartheta_r)L\tilde{\Theta}$$

(2.6a)

$$C = \frac{Lk_s \tan(\beta)}{(\vartheta_s - \vartheta_r)^{\alpha} L^{\alpha}}$$

(2.6b)

the kinematic equation is obtained as follows:

23

$$\frac{\partial \eta}{\partial t} = p - \frac{\partial q}{\partial x} = p - \frac{\partial (C\eta^{\alpha})}{\partial x}$$

(2.7)

where the term C represents local conductivity coefficient, since it depends on soil parameters for a particular position or a particular cell, which encompasses the effects of hydraulic conductivity and slope, to which it is directly proportional, and storage capacity, to which it is inversely proportional.

2.2.4.1.4 Non-linear reservoir model for the soil water in a generic cell

Integrating Equation (2.7) in the soil over the ith DEM grid cell with space dimension is X in meters, it gives:

$$\frac{\partial v_{s_i}}{\partial t} = pX - \left(C_{s_i}\eta_{s_i}^{\alpha_s} - C_{s_{i-1}}\eta_{s_{i-1}}^{\alpha_s}\right)$$

(2.8)

where α_s is a soil parameter assumed to be of the same value for all the cells in the catchment, v_{s_i} is the volume per unit of width stored in the ith cell in m^2, while the last term in equation (2.8) represents the inflow and outflow balance. A subscript s has been introduced to distinguish this soil water equation from the ones relevant to the overland and the drainage network flows and will be kept from now on.

It is quite evident that the coefficients C are no longer the physically measurable quantities which are defined at a point, but rather they represent integral average values for the entire cell, which nonetheless are still strongly related to the measurable quantities.

24

In the TOPKAPI model, the grid cells are connected together by a tree shaped network; water moves downslope along this tree shaped cell network starting from the initial cells (without upstream contributing areas) representing the "sources", and moving downstream toward the outlet.

According to this procedure, and assuming that in each cell the variation of the vertical water content η_{s_i} along the cell is negligible, the volume of water stored into each cell (per unit width) can be related to the total water content η_{s_i}, that is equivalent to the free water volume in depth, by means of the following simple expression:

$$v_{s_i} = X\eta_{s_i}$$

(2.9)

Substituting for η_{s_i} in equation (2.9) and writing it for the "source" cells namely the uppermost cells in each branch, the following non-linear reservoir equation is obtained:

$$\frac{\partial V_{s_i}}{\partial t} = p_i X^2 - \frac{C_{s_i} X}{X^{2\alpha_s}} V_{s_i}^{\alpha_s}$$

(2.10)

Similarly a non-linear reservoir equation can be written for a generic cell, given the total inflow to the cell:

$$\frac{\partial V_{s_i}}{\partial t} = \left(p_i X^2 + Q_{s_i}^u + Q_{s_i}^u\right) - \frac{C_{s_i} X}{X^{2\alpha_s}} V_{s_i}^{\alpha_s}$$

(2.11)

25

where V_{s_i} is the volume stored in the ith cell in m^3, $Q_{o_i}^u$ is the discharge entering the active cell i as overland flow from the upstream contributing area (m^3/s), and $Q_{s_i}^u$ is the discharge entering the active cell as subsurface flow from the upstream contributing area in m^3/s.

2.2.4.1.5 Soil moisture accounting in a grid cell

The solution to Equation (2.11) can be obtained through several either numerical or analytical algorithms, on the known initial and boundary condition for the ith cell. Subsequently, at each time step the soil water balance calculation can be done by Equations (2.12 - 2.14) as follows:

$$Q_{s_i}^d = \left(p_i X^2 + Q_{o_i}^u + Q_{s_i}^u\right) - \frac{V_{s_i}'(t_0 + \Delta t) - V_{s_i}(t_0)}{\Delta t}$$

(2.12)

$$e_{o_i} = \max \left\{ V_{s_i}'(t_0 + \Delta t) - \min\left(V_{s_i}'(t_0 + \Delta t), V_{sm_i}\right), 0 \right\}$$

(2.13)

$$V_{s_i}(t_0 + \Delta t) = \min\left[V_{s_i}'(t_0 + \Delta t), V_{sm_i}\right] - E_a X^2 \qquad (2.14)$$

where Δt is the computational time interval, t_0 is the initial time of the computation step, $V_{s_i}'(t_0 + \Delta t)$ is the solution of Equation (2.11) at the time $t_0 + \Delta t$ in m^3, $Q_{s_i}^d$ is the outflow discharge from the ith cell during the time $t_0 - t_0 + \Delta t$ in m^3/s, e_{o_i} is the saturation excess volume in the ith cell in m^3, V_{sm_i} is the saturated soil water in the ith cell in m^3, E_a is the actual evapotranspiration within Δt calculated by the evapotranspiration model adopted in ARNO model (Todini, 1996) in meters, and $V_{s_i}(t_0 + \Delta t)$ is the water volume stored in the soil in the ith cell at the time $t_0 + \Delta t$.

26

Up to this point it was implicitly assumed that the entire outflow from a cell flows into the downstream cell immediately. However this is not entirely true; in fact the cells can be divided into two groups on the basis of the minimum drained area (threshold) suggested by O'Callaghan and Mark (1984), with a first group where the overland flow is dominant and another one where a channel flow is also present. For the latter cells the outflow is still evaluated by means of the Equation (2.12), but it is then partitioned between the channel and the downstream cell according to a gradient based upon the average slope of the four surrounding cells. This allows the determination of the amount of subsurface flow feeding the drainage channel network. This operation of flow partition is also performed for the overland flow.

2.2.4.2 Surface water and channel flow models

2.2.4.2.1 Kinematic wave formulation for overland flow and channel flow
Since it is assumed that all the precipitation infiltrates into the ground until the soil reaches saturation, the input to the surface water model is the precipitation excess resulting from the saturation of the soil layer.

Overland flow routings are described similarly to the soil component, according to the kinematic approach (Wooding, 1965), in which the momentum equation is approximated by means of the Manning's formula. For a general cell, the kinematic wave approximations of overland flow and channel flow are described in Equations (2.15) and (2.16), respectively:

27

$$\begin{cases} \dfrac{\partial h_o}{\partial t} = r_o - \dfrac{\partial q_o}{\partial x} \\ q_o = \dfrac{1}{n_o}(\tan \beta)^{\frac{1}{2}} h_o^{\frac{5}{3}} = C_o h_o^{\alpha_o} \end{cases}$$

(2.15)

where h_o is the water depth over ground surface in m, r_o is the saturation excess resulting from the solution of the soil water balance equation (2.11), either as the precipitation excess or the ex-filtration from the soil in absence of rainfall, in m/s, n_o is the Manning friction coefficients for the surface roughness in $m^{-\frac{1}{3}}s^{-1}$, $C_o = (\tan \beta)^{\frac{1}{2}}/n_o$ is the coefficient relevant to the Manning formula for overland flow, $\alpha_o = 5/3$ is the exponent which derives from using Manning formula.

$$\begin{cases} \dfrac{\partial h_c}{\partial t} = r_c - \dfrac{\partial q_c}{\partial x} \\ q_c = \dfrac{1}{n_c} s_0^{\frac{1}{2}} h_c^{\frac{5}{3}} = C_c h_c^{\alpha_c} \end{cases}$$

(2.16)

where h_c is the water depth in the channel reach in m, r_c is the lateral drainage input, including the overland runoff reaching the channel reach and the soil drainage reaching the channel reach in m/s, s_0 is the bed slope, assumed to be equal to the ground surface slope $\tan(\beta)$, n_c is the Manning friction coefficients for the channel roughness in $m^{-\frac{1}{3}}s^{-1}$, $C_c = s_0^{\frac{1}{2}}/n_c$ is the coefficient relevant to the Manning formula for channel flow, $\alpha_c = 5/3$ is the exponent which derives from using Manning formula.

28

2.2.4.2.2 Non-linear reservoir model for overland flow and channel flow in a grid cell

In analogy to what was done for the soil, by assuming that the water depth is constant over a cell and integrating the kinematic equation over the longitudinal dimension, it gives the non-linear reservoir model for the overland flow, as in equation (2.17).

$$\frac{\partial V_{o_i}}{\partial t} = r_{o_i} X^2 - \frac{C_{o_i} X}{X^{2\alpha_o}} V_{o_i}^{\alpha_o}$$

(2.17)

where the footer i denotes the ith cell number, V_{o_i} is the volume of the water on the surface in the cell i in m².

KNUST

Similar considerations also apply to the channel network, which is assumed to be tree shaped with reaches of wide rectangular cross sections. In this case the surface width is not constant but it is assumed to be increasing towards the catchment outlet. Under these assumptions, the following expression of non-linear reservoir model can be written for a generic reach:

$$\frac{\partial V_{c_i}}{\partial t} = \left(r_{c_i} X W_i + Q_{c_i}^u \right) - \frac{C_{c_i} W_i}{(X W_i)^{\alpha_c}} V_{c_i}^{\alpha_c}$$

(2.18)

where V_{c_i} is the volume of water stored in the ith channel reach in m³, W_i is the width of the ith rectangular channel reach, which is taken to increase as a function of the area drained by the ith cell (see Equation (2.19)), on the basis of the geo-morphological considerations, $Q_{c_i}^u$ is the inflow discharge from the upstream reaches in m³/s.

29

$$w = w_{max} + \left[\frac{w_{max} - w_{min}}{\sqrt{A_{tot}} - \sqrt{A_{th}}} \right] \left(\sqrt{A_{dr}} - \sqrt{A_{tot}} \right)$$

(2.19)

where w is the generic width, w_{max} is the maximum width, at the basin outlet, w_{min} is the minimum width, corresponding to the threshold area, A_{th} is the threshold area which is the minimum upstream drainage area required to initiate a channel, A_{tot} is the total area and A_{dr} is the generic drained area.

The entire overland outflow from the ith cell and the channel outflow from the ith channel cell can be obtained by using Eqs. (4.20) and (4.21), respectively.

$$Q_{a_i}^d = \left(r_{o_i} X^2 \right) - \frac{V_{o_i}(t_0 + \Delta t) - V_{o_i}(t_0)}{\Delta t}$$

(2.20)

$$Q_{c_i}^d = \left(r_{c_i} X W_i + Q_{c_i}^u \right) - \frac{V_{c_i}(t_0 + \Delta t) - V_{c_i}(t_0)}{\Delta t}$$

(2.21)

2.2.4.3 Evapotranspiration component

Given the information of air temperature, wind speed, humidity, solar radiation, the most complex and physically realistic model for estimating actual evapotranspiration is the Penman-Montieth equation, which has been widely used in many distributed models, e.g. SHE (Abbott et al., 1986 and Abbott et al., 1986), DHSVM (Wigmostra et al., 1994).

30

Although acknowledging the fact that the Penman-Monteith equation is the most rigorous theoretical description for this component, for a practical utilisation a simplified approach is generally necessary because in most countries the required historical data for its estimation are not extensively available.

Evapotranspiration plays a major role not really in terms of its instantaneous impact, but in terms of its cumulative temporal effect on the soil moisture volume depletion; this reduces the need for an extremely accurate expression, provided that its integral effect is well preserved.

In the present TOPKAPI model, evapotranspiration can be either computed externally and directly introduced as an input to the model or estimated internally as a function of the air temperature. A simplified technique in the ARNO model used to calculate the evapotranspiration starting from the temperature and from other topographic, geographic and climatic information is adapted. The effects of the vapour pressure and wind speed are explicitly ignored and evapotranspiration is calculated starting from a simplified equation known as the radiation method (Doorembos et al., 1984).

In the distributed version of the TOPKAPI model, the evapotranspiration is evaluated at the DEM grid scale, while in the lumped version of the model, the evapotranspiration is calculated at the sub-basin or basin level. The air temperature value for a generic DEM grid can be calculated by means of thermal gradient method as shown in Equation (2.22) or by Block Kriging method (de Marsily, 1986; Matheron, 1970).

$$T_i = T_r + 0.006(h_r - h_i)$$

(2.22)

where T_i, h_i are the air temperature and the elevation at i^{th} grid, respectively; T_r, h_r are the air temperature and the elevation of the representative temperature measurement station, respectively. The ith grid resides in the Thiessen Polygon of the representative temperature measurement station.

Potential evapotranspiration is calculated by means of the radiation method, obtained from the Penman-Monteith equation, introducing some simplifications necessary owing to the lack of sufficient data for the rigorous application. The effects of the vapour tension and of the wind speed are neglected. The equation adopted is the following:

$$ET_{0d} = C_v W_{ta} R_s = C_v W_{ta}\left(0.25 + 0.50\frac{n}{N}\right)R_a$$

(2.23)

where ET_{0d} is the reference evapotranspiration, i.e. evapo-transpiration in soil saturation conditions caused by a reference crop (mm/day) ; C_v is an adjustment factor obtainable from tables as a function of the mean wind speed; W_{ta} is a compensation factor that depends on the temperature and altitude; R_s is the short wave radiation measured or expressed as a function of R_a in equivalent evaporation (mm/day); R_a is the extraterrestrial radiation expressed in equivalent evaporation (mm/day); n/N is the ratio of actual hours of sunshine to maximum hours of sunshine (values measured or estimated from mean monthly values).

Hence the calculation of R_S requires both knowledge of R_a, obtainable from tables as a function of latitude, and knowledge of actual n/N values, which may not be

32

available. In the absence of the measured short wave radiation values R_s or of the actual number of sunshine hours otherwise needed to calculate R_S as a function of R_a (see equation (2.23)), an empirical equation was developed that relates the reference potential evapotranspiration ET_{0d}, computed on a monthly basis using one of the available simplified expressions such as for instance the one due to Thornthwaite and Mather (1955), to the compensation factor W_{ta}, the mean recorded temperature of the month T and the maximum number of hours of sunshine N. The developed relationship is linear in temperature (and hence additive), and permits the dissaggregation of the monthly results on a daily or even on an hourly basis, while most other empirical equations are ill-suited for time intervals shorter than one month.

The relation used, which is structurally similar to the radiation method formula in which the air temperature is taken as an index of radiation, is:

$$ET_0 = \alpha + \beta N W_{ta} T_m$$

(2.24)

where ET_0 is the reference evapotranspiration; T_m is the area mean air temperature; N is the monthly mean of the maximum number of daily hours of sunshine (tabulated as a function of latitude); W_{ta} is a weighting factor, for a given sub-basin it can be either obtained from tables or approximated by a fitted parabola.

$$W_{ta} = A\overline{T}^2 + B\overline{T} + C$$

(2.25)

where A, B, C are coefficients to be estimated; $\overline{T}$ is the long term mean monthly sub-basin temperature (°C).

2.2.4.3.1 Estimation of the average monthly potential evapotranspiration according to Thornthwaite

The values of the potential evapotranspiration are computed for a given DEM grid in the distributed TOPKAPI model or a given sub-catchment in the lumped model according to Thornthwaite (1955), by means of the following formula:

$$E_{th}(i) = 16 a(i) \left[10 \frac{T(i)}{b} \right]^c$$

(2.26)

where $E_{th}(i)$ is the average monthly potential evapotranspiration (in mm/month); $T(i)$ is the monthly-average air temperature in °C for i^{th} month; $n(i)$ is the number of days in month i; $N(i)$ is the Mean Daily Duration of Maximum Possible Sunshine Hours, $a(i) = \frac{n(i)}{30} \frac{N(i)}{12}$;

b is the thermal index defined as $b = \sum_{i=1}^{12} \left[\frac{T(i)}{5} \right]^{1.514}$; and

$c = 0.49239 + 1792 \times 10^{-5} b - 771 \times 10^{-7} b^2 + 675 \times 10^{-9} b^3$.

2.2.4.3.2 Calculation of actual evapotranspiration

The calculated potential evapotranspiration is corrected as a function of the actual soil moisture content, to obtain the actual evapotranspiration:

$$\begin{cases} ET_a = ET_0 \dfrac{V}{K_p V_{sat}}, & V < K_p V_{sat} \\ ET_{ea} = ET_0 & otherwise \end{cases}$$

(2.27)

where V is the actual volume of water stored in the soil, V_{sat} is the local saturation volume, K_p is the percentage of the saturation volume, to be fixed. The K_p factor is related to the presence and the type of vegetation, therefore it is assumed that it takes

34

into account also the phenomenon of the canopy interception, not explicitly represented.

CHAPTER THREE

3 STUDY AREA

3.1 The Pungu Experimental Site

In investigating and understanding the hydrologic behavior of the Volta Basin, three pilot sites were selected for intensive observation of several hydro-ecological processes in the Ghana side of the catchment by the Glowa-Volta Project. The selected areas are Ejura in the Ashanti Region which falls within the middle belt, Tamale in the Northern Region and Navorongo in the Upper East Region which falls within the northern part of Ghana. This study was carried out at the Navrongo site in a small village called Pungu, 8 km North of Navrongo in the Kassena-Nankana District of the Upper East Region of Ghana and is located within latitudes 10° 54' N and longitude 1°03' W. Figure 3-1 presents the geographical location of the Kassena-Nankana District relative to the boundaries of Ghana and that of the Volta Basin. In Figure 3-2, the geographical location of the experimental site in the Kassena-Nankana District is presented. The area covered in this study is approximately 8.98 km².

The population of the Kassena-Nankana district is slightly less than 1% of Ghana's population and about 15% of the total population of the Upper East region. The population density is 84 persons per sq. km. The district is largely rural, with only 9.5% living in urban areas. Subsistence agriculture is the mainstay of the district's economy, complemented to some extent by retail trading. About 90% of the people are farmers. The major agricultural products are groundnuts, millet, guinea corn, rice,

36

sorghum, sweet potatoes, beans and tomatoes. Rearing of cattle, goats, sheep, pigs, fowls and guinea fowls also form part of the agricultural activities. Unfortunately, the rainfall pattern limits food cultivation to a single growing season and even though the Tono irrigation dam and a few dugout wells supply water for dry season farming, the major crop grown during this time is tomato. Weather conditions in the district can be very severe, resulting in either occasional floods or droughts and, therefore, poor harvest (Binka et al, 1999).
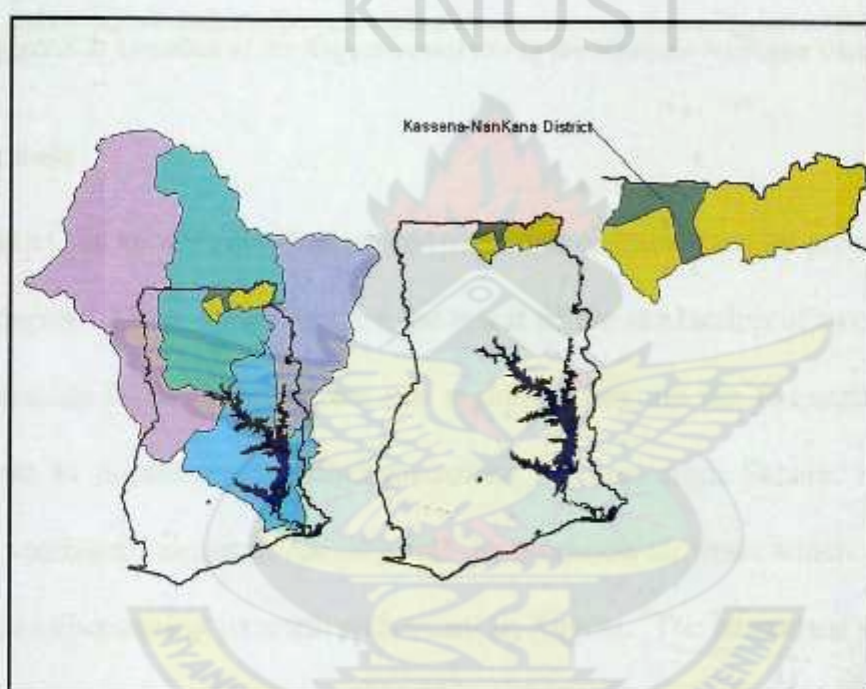
Figure 3-1: Location of the Kassena-Nankana District in the Volta Basin
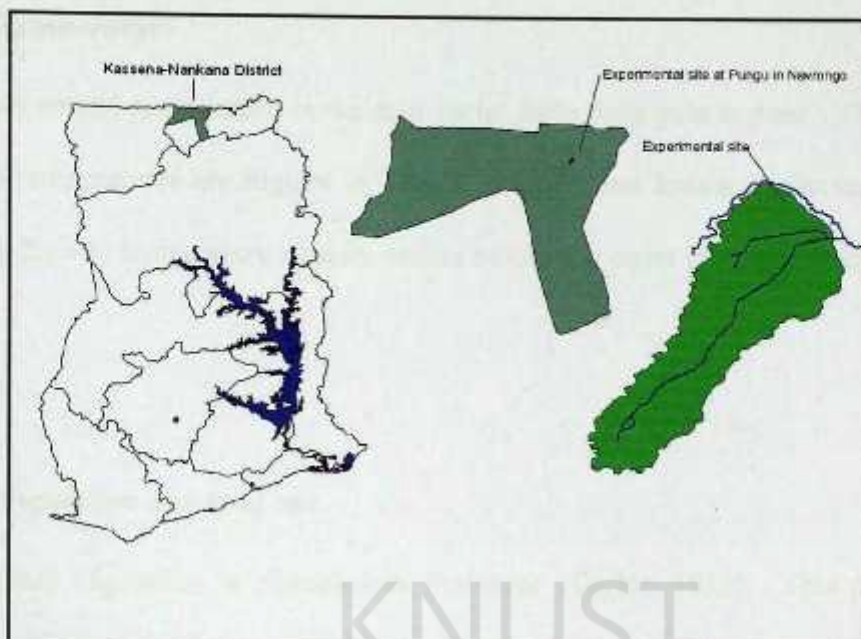
Figure 3-2: Location of the Experimental site in the Kassena-Nankana District

3.1.1 Climate

The climate of the area is classified as Sudanese and characterized by pronounced wet and dry seasons. These conditions are the result of the interaction of two air masses that predominate in the West Africa sub region. They are the harmattan air mass which blows in north-easterly direction across the area from Sahara, reaching its maximum southward extent in January and the monsoon air mass which passes over the area and experiencing its north end extent in August. The harmattan air is warm, dry and dusty whereas the monsoon air is warm, humid and wet.

3.1.2 Rainfall

The area has a uni-modal wet season which starts from March and reaches its peak in August. The monthly totals increase gradually from April to August. The monthly totals then fall sharply. The average annual rainfall of Navrongo is about 900 mm.

3.1.3 Temperature

The mean annual temperature in the area varies little from year to year. The average monthly temperatures are highest in March ($40.0^{\circ}C$) and lowest in December ($20.0^{\circ}C$). The highest temperature usually occurs before the onset of the rains in March or April.

3.1.4 Vegetation and land use

The original vegetation is classified as Sudanese (Taylor, 1952). This consists of short deciduous trees often widely spaced and a ground flora composed of different species of grasses of varying heights. Due to human activities like settlement, over population, annual and periodic fires many areas are now degraded. The areas suitable for agriculture is cultivated to arable crops mainly sorghum, millet, maize, groundnut, bambarra beans and cowpea. The farms are mostly located within one to two kilometers radius of the settlements. Sheep and goats rearing are also carried-out on the various farmsteads. The animals are kept indoors during the farming season but allowed to graze freely in the field during the dry season.

3.1.5 Relief and drainage

Generally the area is gentle sloping (2-5%) with slopes of about a kilometer long. The catchment is drained by the Budunga stream and its tributaries in South-North direction.

39

3.1.6   Geology

The soils of the Pungu area are developed over hornblende granite which is medium grained with a lot of feldspar which is commonly pink colored.

3.1.7   Relative Humidity

The relative humidity figures are usually high in the rainy season, particularly from July to September and low in the dry harmattan period from December to March.

4 METHODOLOGY

4.1 Field Activities

The study area is one of the test sites selected for intensive observation and monitoring of agro-eco-hydrological variables within the scope of the overall Glowa Volta Project objectives.

4.1.1 Hydro-meteorological Data

Instruments at the site include an automatic weather station, which records all weather variables (rainfall, minimum and maximum temperature, net radiation, relative air humidity, barometric pressure, wind speed and direction, and soil heat flux). These parameters are logged every 10minutes by a Campbell CR10 data logger. The site is also equipped with a scintilometer set to capture the heat flux in the catchment transects. Two additional tipping bucket rain gauges equipped with HOBO data loggers were also installed. The cumulative number of tips were converted into millimeters of rainfall using the Hobo BoxCar Pro 4.3 (User Guide (2002)). A 90° V-notch weir equipped with Van Essen pressure transducer divers, which measures water level, was installed to obtain the observed runoff.

4.1.2 Transect Creation

To enable soil data collection at a regular intervals, a baseline of approximately 2 km long was created due north-east and south-west at 10° 55′ 21.9″ N, 01° 02′ 45.7″ W and 10° 54′ 33.6″ N, 01° 03′ 19.8″ W respectively. This was then divided into strips

strips by running parallel traverses at right angles to the baseline at 100-m intervals. Pegs were put at 50-m intervals along the traverses up to 200-m on each side of the baseline, resulting in rectangular grid of 100 × 50 meters.

4.1.3 Soil Sampling and Analysis

At the pegged points, disturbed and undisturbed soil samples were collected from the topsoil to a depth of about 15-cm. The undisturbed samples were taken using a 10.0 cm long by 8.3 cm diameter cylindrical metal core with the help of a ring holder. The sampling core was inserted into the ring holder, which was then inverted onto the soil. The handle of the holder was then tapped gently with a mallet until the top of the soil core was about 0.5 cm below the soil surface. The soil around the holder was then dug, the soil sample core brought out and excess soil cut off with a soil knife. All disturbed soil samples were air dried, sieved and analyzed for particle size distribution. The undisturbed soil samples were analyzed for saturated hydraulic conductivity.

4.1.3.1 Saturated Hydraulic Conductivity

Saturated hydraulic conductivity is the measure of the soil's ability to transmit water under saturated conditions (Klute and Dickson, 1986). Saturated hydraulic conductivity is a very crucial parameter used in determining infiltration, irrigation practice, drainage design, runoff, groundwater recharge and in simulating leaching and other agricultural and hydrological processes. Saturated hydraulic conductivity can be found directly by measuring water movement through a soil sample, or indirectly, by estimating from associated soil properties. Methods that measure

42

saturated hydraulic conductivity directly can be divided into two categories, (1) laboratory techniques, and (2) field techniques. Klute and Dirksen (1986) stated that choosing a method for determining hydraulic conductivity depends on such factors as available equipment, nature of the soil, kind of samples available, the skills and knowledge of the experimenter; the soil-water suction range to be covered; and the purpose for which the measurements are being made.

The core sample method determines saturated hydraulic conductivity on samples by either a constant head or a falling head test. In this study, the falling head test method was employed.

In the falling head test, the hydraulic conductivity is determined from the rate of change of velocity of a falling water column. The core samples which were taken in the field were kept from drying. In the laboratory, the samples were saturated from the bottom to prevent air entrapment. The saturated hydraulic conductivity (Ks) measurements were made on 10.0 cm long by 8.3 cm diameter core samples in the laboratory using the falling head method developed by Klute and Dirksen (1986). The soil in the core is held in place with a fine nylon cloth, tied with a rubber band and soaked in water for 24 hours or until saturated. The soaked soil is fitted with another cylinder of the same diameter but of 40 cm height at the top of the core to allow imposition of a hydraulic head. A large metallic box with perforated false bottom is fitted with fine gravel (<2 cm). A fast filtration filter is placed on the soil core. With the core placed on the gravel box, water is gently added to the core to give a hydraulic head in the extended cylinder. The water then flows through the soil and is collected in the box and drained off by plastic pipe tubing. The fall of the hydraulic head, h_t at

the soil surface was measured as a function of time t using a water manometer with a meter scale. Plate 4-1 presents a typical laboratory setup of the falling head test method. Note: Enough time must be allowed for water to flow through the soil to ensure uniform flow. Saturated hydraulic conductivity was calculated by the standard falling head equation:

$$K = \frac{aL}{A(t_2 - t_1)} \ln \frac{h_t}{h_0}$$

(4.1)

where L is the length of the soil core, A is the cross-sectional area of the sample core, a is the cross-sectional area of the cylinder, h_t is the height of the water column at time t, and h_0 is the height of the water column at time $t = 0$.

Since $a = A$, rearranging equation 4.1, a regression of $\ln \frac{h_t}{h_0}$ against t with slope b:

$$K = bL$$

(4.2)

Table 4-1: Saturated hydraulic conductivity classification values

Description	Saturated Hydraulic Conductivity (cm/h)
Very slow	< 0.8
Slow	0.8 – 2.0
Moderate	2.0 – 6.0
Moderately rapid	6.0 – 8.0
Rapid	8.0 – 12.5
Very rapid	> 12.5

Source: Landon, 1991

44

Plate 4-1: Hydraulic conductivity analysis by falling head test

4.1.3.2 Particle Size Distribution: the hydrometer method

The soil particle size and its mineralogical composition largely determine the nature and behavior of soil, i.e., internal geometry and porosity, its interactions with fluids and solutes, as well as compressibility, strength, and thermal regime (Hillel, 1998). The amount of each particle size group (sand, silt, or clay) in a soil is known as the soil particle size distribution. There are different ways of analyzing soil texture, namely sieving, pipette and the hydrometer methods. In this study, the hydrometric method was used. This involved the removal of organic matter by adding a chemical dispersing agent (sodium hexametaphosphate) after which the sample was mechanically agitated through shaking for complete dispersion of soil floccules. The hydrometer was then used to determine the density of the solution at timed settling increments. The density of the solution was then used to determine the concentration percentages for sand and clay particles. For the determination of sand and clay size fractions, Stokes' Law relationship between the diameter of suspended particles and their rate of settlement in liquid at constant temperature was used.

45

The percentages of sand, silt, and clay were calculated and the textural class name was determined for each soil sample. The soils were classified into different textural classes using the USDA textural triangle. This textural triangle is a diagram that shows how each texture is classified based on the percent of sand, silt, and clay in each soil sample.

The results of the soil textural analysis were then imported into the Integrated Land and Water Information System (ILWIS) GIS software for geospatial analysis. Spatial correlation and Semi-variogram analysis were performed prior to ordinary kriging to obtain a raster soil map.

4.1.4 Land Use Type

Of particular interest in this study is the effect of changes in land use pattern on surface runoff, the importance of topography associated with the effect of tillage practice and soil properties in controlling the magnitude and distribution of surface runoff. The boundaries of the various land uses at the site were registered by generating codes in the HP 2341 handheld device of the Differential Global Positioning System (DGPS), Ashtech Locus equipment (Ashtech, 1998a) during the topographic survey. These codes were then imported into ArcView 3.3 (ESRI, 1992-2000) platform where the boundaries of the various land uses were delineated.

4.1.5 Terrain Analysis (DEM Generation)

There are three main sources of topographic data: surface-specific point elevation, contour and streamline, and remotely sensed elevation data. These data can be

elevation model (DEM)), triangulated irregular network (TIN), and contours. The choice of one method over the other is usually a question of preference and/or source of data (Moore et al., 1991 and Wilson and Gallant, 2000).

In this study, a Differential Global Positioning System (DGPS), Ashtech Locus equipment (Ashtech, 1998a), was used to generate point measurements at intervals of 10 meters. This was done by first creating a control (base) site at which one of the satellite antennas was mounted on a tripod. Plate 4-2 presents the setting up of the antennas on the tripod before synchronization. The two antennas were synchronized using the HP 2341 handheld device and data recorded at 15-seconds intervals (see Ashtech Locus manual for details (Ashtech, 1998)). The second antenna (the rover) was then mounted on a range pole. Each data set was checked and the procedure repeated until the entire basin was covered. During the field topographic survey, at specific locations where changes in land use was noticed, site identification codes were recorded. These codes were later used to develop the land use map.

Plate 4-2: Field surveys with the Differential Global Position System

The data was processed using the Locus processor 1.2 (Ashtech, 1998b). The processing was carried out using Clark 1880 Modified parameters as provided by the Survey Department of Ghana. In the absence of World Geodetic System (WGS) 1884 control points, a control point was created and data taken at this point in the static mode for three hours to insure accuracy. The data quality was checked using the Locus processor 1.2 (Ashtech, 1998b), and site coordinates with failed quality assurance (QA) and high standard error (i.e., > 10) were not used for the DEM development. The data was reprocessed and then adjusted to improve the site coordinate quality and reliability. Geospatial analyses were then carried out on the point data prior to a kriging interpolation using the Integrated Land and Water Information System (ILWIS) software (ITC and RSG/GSD, 2002) to obtain a DEM of grid cell size of 10 m.

4.2 Model Calibration, Evaluation and Application

4.2.1 Model Calibration

The TOPKAPI model uses information derived from the soil, land-use and topographic (DEM) maps in raster format and meteorological variables such as rainfall, temperature and sunshine duration as input data. The DEM, land-use and soil maps were obtained through field surveys.

4.2.1.1 DEM Map elaborations

The application of DEM data in the TOPKAPI model consists of generating drainage network, drainage direction and the steepness of each grid cell. It comprises three steps as follows:

- Identify and correct sinks and false outlets

- Identify the connections among the cells, by means of which it is possible to identify the flow pathways, to calculate the steepness for each grid cell

- Identify the channel network given a user-defined minimum drainage area

The drainage network was extracted automatically from the DEM by setting a threshold for the drained area at 1.8% of the total area whereas the minimum and maximum width for the drainage network was set at 0.5 m and 5 m respectively. The generated stream network in raster format was compared with a vector stream network obtained by the surveys. Figure 4-3 below presents the comparison between the generated river network and the existing river network of the site.
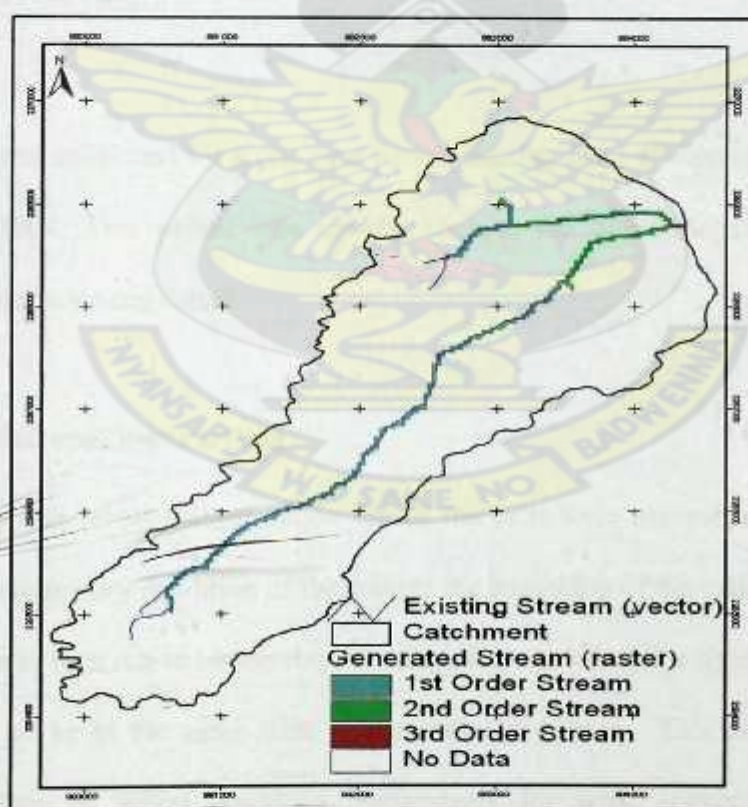

Figure 4-1: Comparison of stream generated by model in raster format and the existing stream in vector format

4.2.1.2 Choice of calibration period

Although physically based, the model still needs calibration because of the uncertainty of the information on the topography, soil characteristics and land-use. Nonetheless the calibration of the TOPKAPI parameters is more an adjustment rather than a conventional calibration.

The initial parameter values of the three basic components in the TOPKAPI model, namely the soil water component, surface water component and channel water component were obtained from the results of the field observations and the literature. The thickness of the soil layer was also obtained from the soil sampling. In calibrating the model, only the surface and channel roughness were modified. The final parameter values were obtained by 'trial and error' by comparing the model output with the observed runoff.

The model was calibrated for a one year period starting from 1st January 2004 to 31st December 2004. This period was chosen because the hydro-meteorological data collection was more consistent.

4.2.1.3 Initial conditions setting

In this study, the initial soil saturation for all the cells were assumed to be constant due to the extreme dry condition of the soils at the beginning of the calibration period. The model was then run to obtain the soil saturation condition at a time when the soil is supposed to be in the same state as the initial condition. This procedure gives realistic values of initial condition, particularly for what concerns the spatial distribution of the saturation percentage. At the initial conditions, it is assumed that no

50

surface water are over the slopes; the water depth in a generic channel cell increases as a function of the channel width at the outlet channel reach and the area drained by the channel.

4.2.2 Model Evaluation

The ability to reproduce the observed runoff hydrograph was evaluated using the coefficient of efficiency (Ce) defined by Nash and Sutcliffe (1970) as:

$$Ce = 1 - \frac{\sum_{i=1}^{n}(Q_{oi} - Q_{si})^2}{\sum_{i=1}^{n}(Q_{oi} - Q_{m})^2}$$

(4.3)

where Q_{oi} is the observed runoff discharge at time i, Q_{si} is the simulated runoff at time i, Q_m is the mean observed runoff and n is the number of time step in the computation. $Ce=1$, indicates a perfect agreement between the simulated and the observed hydrograph for the period under consideration. It must however be mentioned that this is rarely possible in view of certain assumptions often used in model simulation runs which often do not adequately represent field conditions. The more the value of Ce slides away from 1, the lesser the goodness of fit, and a negative value implies that the observed mean is a better estimate than the simulated value (Esteves et al, 2000).

The model was also evaluated by using the coefficient of determination, R^2 by plotting all the estimated runoff for the calibrated period against the observed runoff. $R^2=1$ indicates a perfect agreement between the measured and estimated hydrographs.

4.2.2.1 Model Sensitivity

The distributed-parameter approach permits several structural attributes of the model to be varied in a controlled fashion. However, in this study, a simple sensitivity analysis and a simple sensitivity index equation (Cullmann et al, 2006), equation 4.4, were applied to the surface and channel roughness coefficients. All other parameters such as the meteorological variables, hydraulic conductivity and soil layer thickness were held constant since they were directly obtained from field measurements. In the simple sensitivity analysis, only one parameter was varied uniformly by -50% to +50% of parameter value. The sensitivity analysis was carried out with respect to the peak flow. The simple sensitivity index (Cullmann et al, 2006) is given by:

$$S = \frac{(P(+10\%) - P(-10\%))}{P}$$

(4.4)

Where S is the measure of sensitivity, P+10% is the peak discharge of the considered flow hydrograph for parameter +10%, P−10% is the peak discharge of the considered flow hydrograph for parameter −10% and P is the peak discharge of the considered flow hydrograph for the simulated parameter set.

4.2.3 Model Application

In line with the specific objectives of this study, the calibrated TOPKAPI model was applied at the experimental site to evaluate the impact of possible land-use changes on the rainfall-runoff process. The model was also applied to the Nabogo catchment, a sub-catchment of the Volta basin to generate runoff data to fill-in gaps in the hydrological data set.

4.2.3.1 Land-use scenarios

Spatial variability of land-use has been cited as the basis of the observed differences in runoff response using analytical or model-based evaluation. However, the hydrologic effect of alteration in land-use at a watershed scale is still an unresolved problem and is now a primary concern of most developing countries, which are commonly experiencing changes in lad-use patterns caused by increasing populations and its attendant demand for land.

After the performance of the calibrated model was evaluated by comparing the observed and simulated flows, the model was applied to evaluate the effects of land-use change on the mean annual runoff and percentage of saturation in the experimental site. Proportional changes in two classes of land-use (cultivated and uncultivated) within the watershed were derived by artificially increasing the area under cultivation by 20%, 40%, 60% and 80% of the uncultivated area and vice versa.

4.2.3.2 Data in-filing in the Nabogo sub-catchment

Taking advantage of the fact that, the TOPKAPI model is a physically based model, and only has a few parameters to be calibrated, it was used in this study as a tool to convert available data on rainfall, temperature, topography, land-use and soil maps into runoff at the outlet of the Nabogo catchment.

4.2.3.2.1 The Nabogo catchment

The Nabogo catchment is one of the sub-catchments of the Volta basin. The catchment has an estimated area of 2086 km^2 with a varying elevation ranging from 91 m to 411 m above mean sea level.

The basin topography is represented by a DEM (Figure 4-2) based on a 1: 50,000 contour map obtained from the Ghana Survey Department. The contour map was interpolated into a kilometer grid size DEM using kriging interpolation operation in the Integrated Land and Water Information System (ILWIS) software (ITC and RSG/GSD, 2002).

The land-use and soil maps of the basin were obtained from the Ghana - country at a glance, G-CAG data set in vector format. The vector maps were converted into raster format (Figure 4-3 and 4-4) using the grid operation in ArcView 3.3 (ESRI, 1992-2000). The dominant land-use in the basin is open cultivated savanna woodland (11-20 trees/ha) while the least land use is closed savanna woodland (>25 trees/ha), Table 4-2. Planosols forms the largest soil properties covering 39.02% in the basin while leptosols forms the least with just 2.83%, Table 4-3.
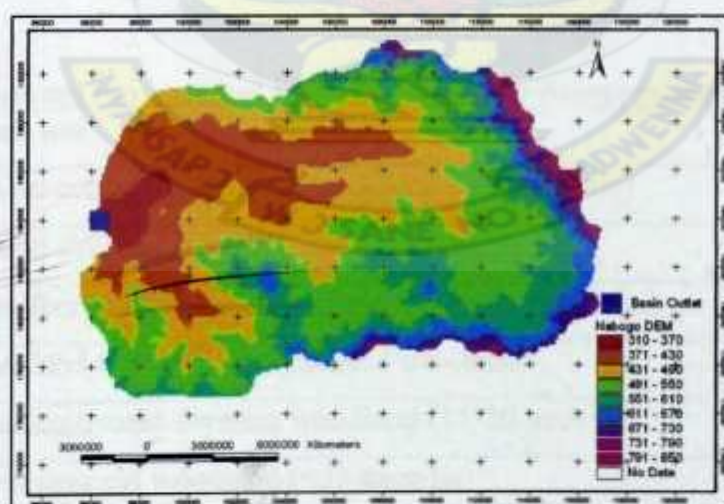

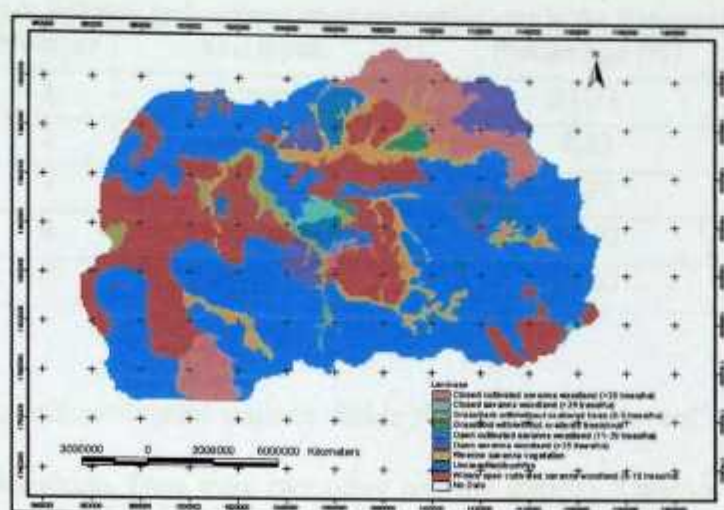Figure 4-2: DEM of the Nabogo catchment

Figure 4-3: Land-use map of the Nabogo catchment
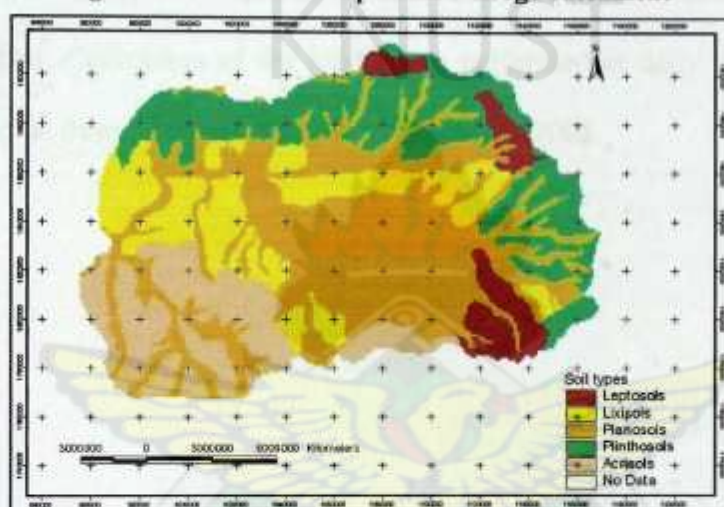
Figure 4-4: Soil map of the Nabogo catchment

Table 4-2: Land-use and corresponding percentage area in the Nabogo catchment

Number	Land use	Percentage (%)
1	Closed cultivated savanna woodland (>20 trees/ha)	2.79
2	Closed savanna woodland (>25 trees/ha)	0.08
3	Grass/herb with/without scattered trees (0-5 trees/ha)	0.36
4	Grassland with/without scattered tree/shrub	0.06
5	Open cultivated savanna woodland (11-20 trees/ha)	82.60
6	Open savanna woodland (<25 trees/ha)	0.76
7	Riverine savanna vegetation	0.63
8	Unclassified/bushfire	0.22
9	Widely open cultivated savanna woodland (6-10 trees/ha)	12.50

Table 4-3: Soil type and corresponding percentage area in the Nabogo catchment

Number	Soil types	Percentage (%)
1	Acrisols	21.71
2	Leptosols	2.83
3	Lixisols	6.37
4	Planosols	39.02
5	Plinthosols	30.07

There are two meteorological stations within the Nabogo catchment located at Pong-Tamale and Savelugu. Data from two other near-by stations, Daboya and Garu were added to calculate the areal distribution of rainfall and temperature using the Thiessen polygon method. Calibration of the model was performed at daily time step using hydrological data from 1st March 2001 to 28th February 2005.
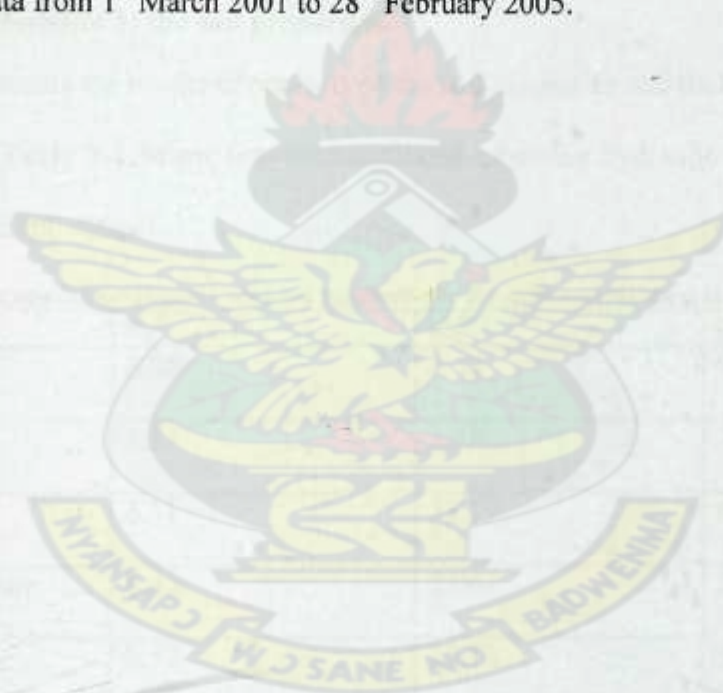
5   RESULTS AND DISCUSSIONS

5.1   Field Results and Discussions

In this section, the general characteristics of soil properties, terrain attributes and

distribution of soil properties of the study sites are outlined. The soil properties

considered here include particle size distribution (sand, silt and clay), and saturated

hydraulic conductivity (Ks); the terrain parameters are elevation and slope.

5.1.1   Characteristics of the soil properties

This section presents the results of analysis of the soil properties and their variation at

the study site. Table 5-1 below lists recommended saturated hydraulic conductivity

for different textural classes.

Table 5-1: Recommended saturated hydraulic conductivity for different textural classes.

Soil Texture	K_s^a	K_s^b	K_s^c
Clay	0.06	0.44	0.48
Loam	1.32	2.78	1.68
Loamy sand	6.11	38.19	6.30
Sandy clay loam	0.43	2.06	2.28
Sandy loam	2.59	11.12	3.01

Source: [a]Rawls et al (1982), [b]Clapp and Hornberger (1978) and [c]Cosby et al (1984)

Descriptive statistics of the soil properties are presented in Table 5-2. The soil at the

study site was found to contain a mean texture (based on the USDA Textural

Triangle) of sandy loam and is dominated by sandy loam, loamy sand, sandy clay loam, loam and clay in decreasing order of distribution (see Table 5-3).

Table 5-2: Descriptive statistics of soil properties

Soil Properties	Minimum	Maximum	Mean	Standard Deviation	Coefficient of Variation (%)
Sand (%)	28	85	71.59	9.60	13.41
Clay (%)	1	50	8.34	7.48	89.75
Silt (%)	10	47	20.08	6.09	30.34
Hydraulic Conductivity (cm/h)	0.05	8.15	4.34	1.86	118.90

The clay content has the largest coefficient of variation (CV) amongst the different particle size distributions. The high CV of clay in the soil may be the result of different land use practices and erosion resulting in sediment deposition in low-lying areas. The Ks had the highest CV of 89 % in the soil (Table 5-2) which is within the range of 86 – 190 % observed by Warrick and Nielson (1980) when they compared the results of measured saturated hydraulic conductivity from different authors. Expressing the Ks in terms of textural classes however shows a low CV, ranging from 4 % to 24 % in the soil (Table 5-3). The soil also has a mean saturated hydraulic conductivity of 4.34 cm/h which indicates a characteristically moderate flow regime in the soil (see Table 5-1 for hydraulic conductivity classification). The mean of the measured saturated hydraulic conductivity values for the different soil textural classes at the study area were within ranges as given by Rawls et al (1978), Clapp and Hornberger (1978), and Cosby et al (1984).

Table 5-3: Saturated hydraulic conductivity of the soil based on the USDA textural classification

Soil Texture	Percentage Soil	Mean Ks (cm/h)	Standard Deviation	Coefficient of Variation (%)
Sandy Loam	47.45	3.30	0.80	24.20
Loamy Sand	43.36	6.26	0.96	15.34
Sandy Clay Loam	6.47	2.17	0.18	8.09
Loam	2.72	1.59	0.07	4.09

5.1.2 Soil Map

The soil map for the site was created using the kriging interpolation operation in ILWIS. Prior to the kriging operation, spatial correlation analysis was performed to obtain the kriging parameters of 1.45 for the nugget, 50 for the sill and 1000 for the range. Figure 5-1 presents the soil map of the site whereas Figure 5-2 presents the spatial variation of the saturated hydraulic conductivity. It can be seen from the latter that, the up-stream portions of the experimental site has high hydraulic conductivity than that of the downstream portions.
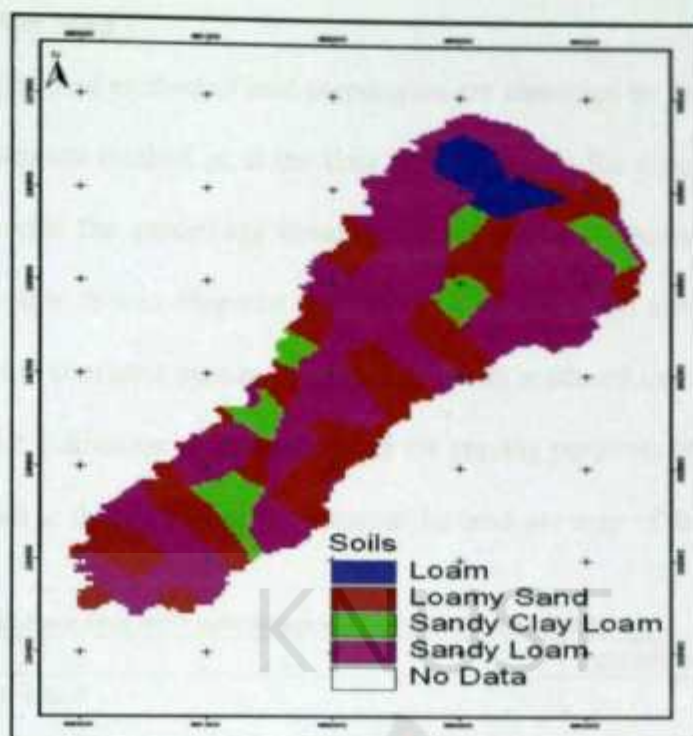
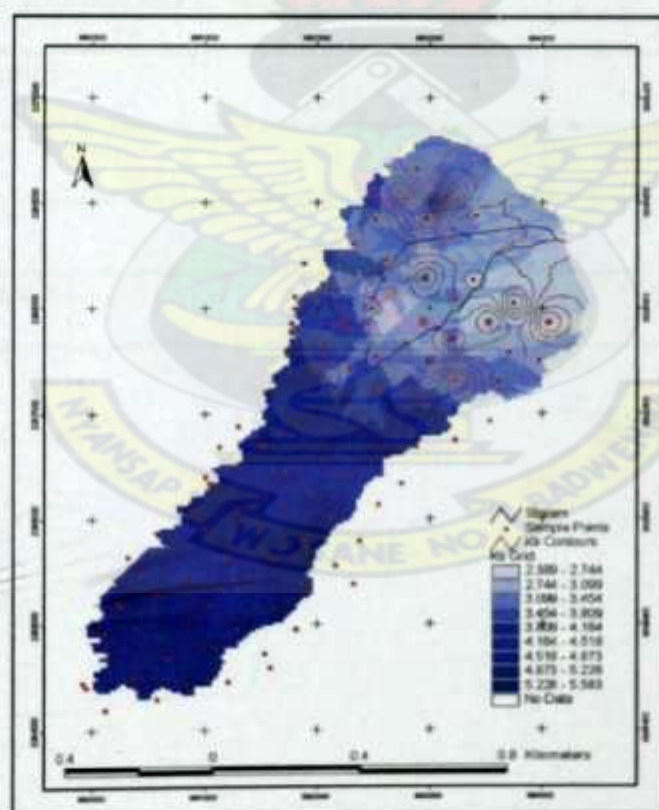**Figure 5-1: Soil map showing the different soil textural classes at the site**

Figure 5-2: Spatial variation of saturated hydraulic conductivity

5.1.3 Land Use Map

The land-use type and method of land preparation are identified by the cultivated crop and land preparation method as at the time of undertaking the topographic surveys. Table 5-4 presents the percentage coverage of the different land-uses as observed during the surveys. It was observed that 60 % of the surveyed area at the site was uncultivated, and consisted mainly of grass/herbs with scattered trees. Either the area is unsuitable for cultivation and therefore left for grazing purposes or exhausted land, intentionally left to fallow. Figure 5-3 presents the land-use map of the site.

Table 5-4: Land use type with percentage coverage at the site (2006)

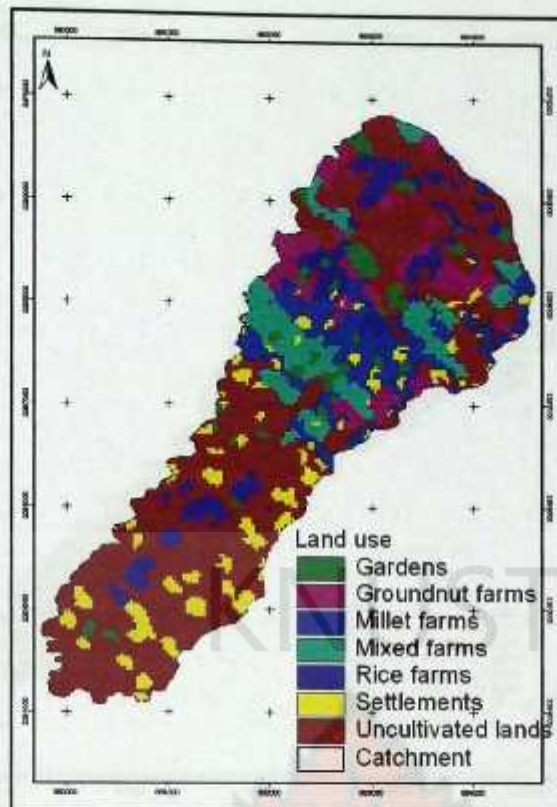| Land use	Percent coverage (%)
Uncultivated Land	60.13
Millet Farms	11.39
Mixed Farms of Groundnut & Millet	8.29
Groundnut Farms	7.99
Rice Farms	5.83
Settlements	3.31
Vegetable Gardens	3.06

Figure 5-3: Land use map of the site

5.1.4 Digital Elevation Model (DEM)

This section presents the results of the terrain analysis. As mentioned earlier, elevations data at several points were kinematically collected using ASHTEC Differential Global Positioning System (DGPS). The obtained data was used to generate a digital elevation model (DEM) of the study site. The study site can be classified as a medium to low land with an average slope of 12.04%, an elevation varying between 181 and 230 meters and a mean elevation of 214.246 meters above sea level (see Figure 5-4 for resulting DEM and Table 5-5 for descriptive statistics).
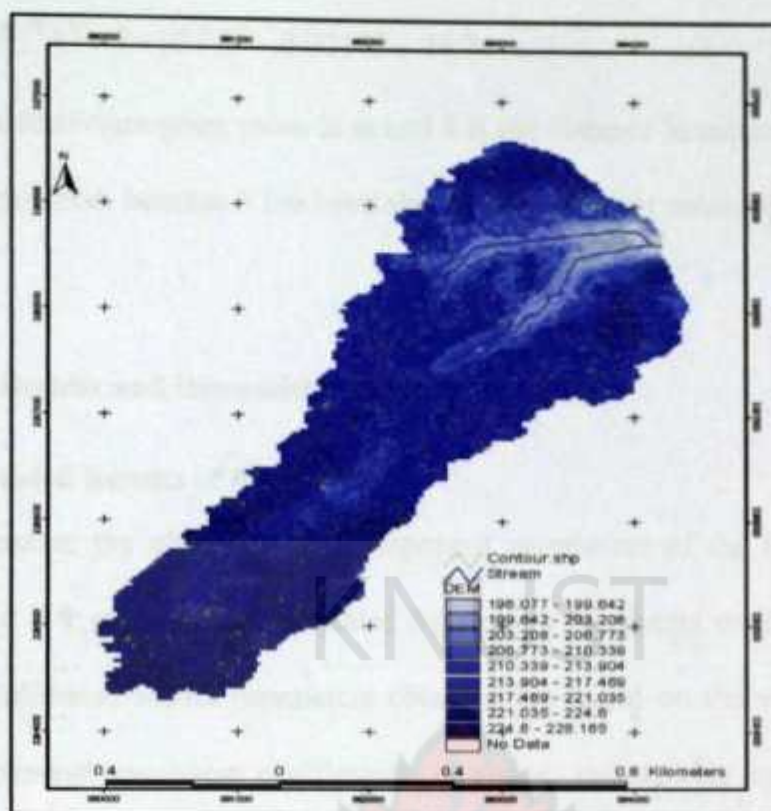
Figure 5-4: Digital elevation map of the study site

Table 5-5: Descriptive statistics of the terrain data at the study site

Number of points	Minimum elevation	Maximum elevation	Mean elevation	Standard deviation	Coefficient of variation
5390	196.077	228.165	214.246	7.529	3.51

The area of the study site as estimated from the survey data was 8.98 km^2. The digital

elevation model was developed with 5390 GPS measurements over the entire

catchment by Kriging interpolation. The first step in Kriging interpolation involves

modeling the spatial structure of the elevation data using the semi-variogram. The

semi-variogram is a function of distance (lag) separating data points. With n number

of observation, there are $\dfrac{(n-1)n}{2}$ unique data pairs. The empirical variogram is

computed as half the average of the squared difference of all data pairs (Chilés et al.,

1999). The experimentally derived variogram was used to fit a polynomial model of

the form:

63

$$q(h) = -6 \times 10^{-10} h^3 + 9 \times 10^{-6} h^2 - 0.0017h + 24.74 \qquad (5.1)$$

where q is the semi-variogram value in m and h is the distance in meters. Kriging was used for interpolation, because it has been shown to be the best unbiased estimator.

5.2 Model Results and Discussions

5.2.1 Calibrated Results of the Model

Table 5-6 presents the observed soil component parameters of the model whereas Table 5-7 and 5-8 presents the calibrated Manning's roughness coefficients of the model. The calibrated model parameters obtained are based on the variation of the surface and channel roughness coefficients, n_s and n_c respectively by the so-called "trial and error" method.

Table 5-6: Soil component parameters obtained through field surveys

Soil Texture	Ks (m/s)	L (m)
Sandy Loam	9.17×10^{-6}	0.15
Loamy Sand	1.74×10^{-5}	0.15
Sandy Clay Loam	6.03×10^{-6}	0.15
Loam	4.42×10^{-6}	0.15

Table 5-7: Calibrated surface component parameters

Land use	n_s
Uncultivated Land	0.150
Cultivated	0.320
Settlements	0.110

Table 5-8: Calibrated channel component parameters

Strahler's Channel Order	n_c
I	0.045
II	0.040
III	0.030

Where k_s is the saturated hydraulic conductivity in m/s, L is the thickness of the soil layer in meters, n_s and n_c are the surface and channel Manning's roughness coefficients in $m^{-1/3}s^{-1}$.

Figure 5-5 presents a comparison of the observed and simulated hydrographs. Comparison of the two hydrographs suggests that the magnitude of simulated peak discharge is slightly lower during the onset of the rainfall-runoff process but slightly higher after the occurrence of the highest peak flow. Detail inspection of the hydrographs also shows that the low flows were not well simulated by the model. This may be due to the fact that percolation was not accounted for in the model.
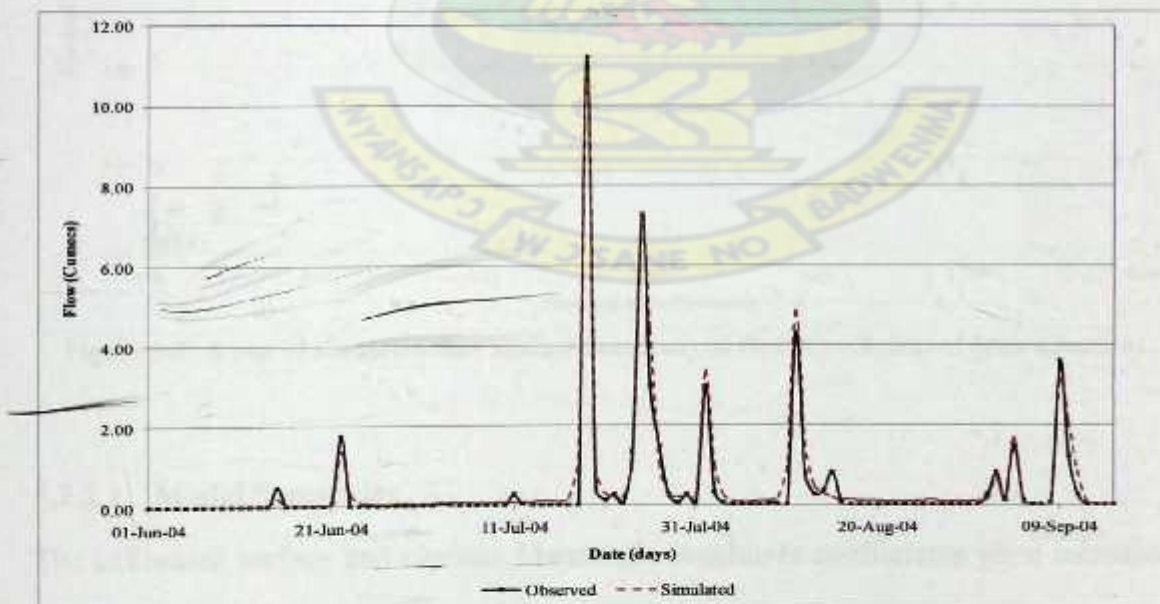

Figure 5-5: Comparison of observed and simulated discharge at the study site

65

5.2.2 Model Evaluation

The coefficient of determination, R^2 which was used to evaluate the performance of the model was found to be 0.929. Figure 5-6 shows a plot of the simulated verses the observed runoff. The high value of R^2 indicates a good correlation between the model output and the measured runoff. Although the R^2 value obtained was high, this was mostly relative to the peak flows as observed in Figure 5-6. The model was also observed to predict the observed hydrograph with an accuracy of 0.877 according to the Nash-Sutcliffe criterion of coefficient of efficiency, Ce. An efficiency of 1 indicates a perfect agreement between the simulated and measured hydrographs. However, a value of Ce further away from 1 indicates a poor goodness of fit.
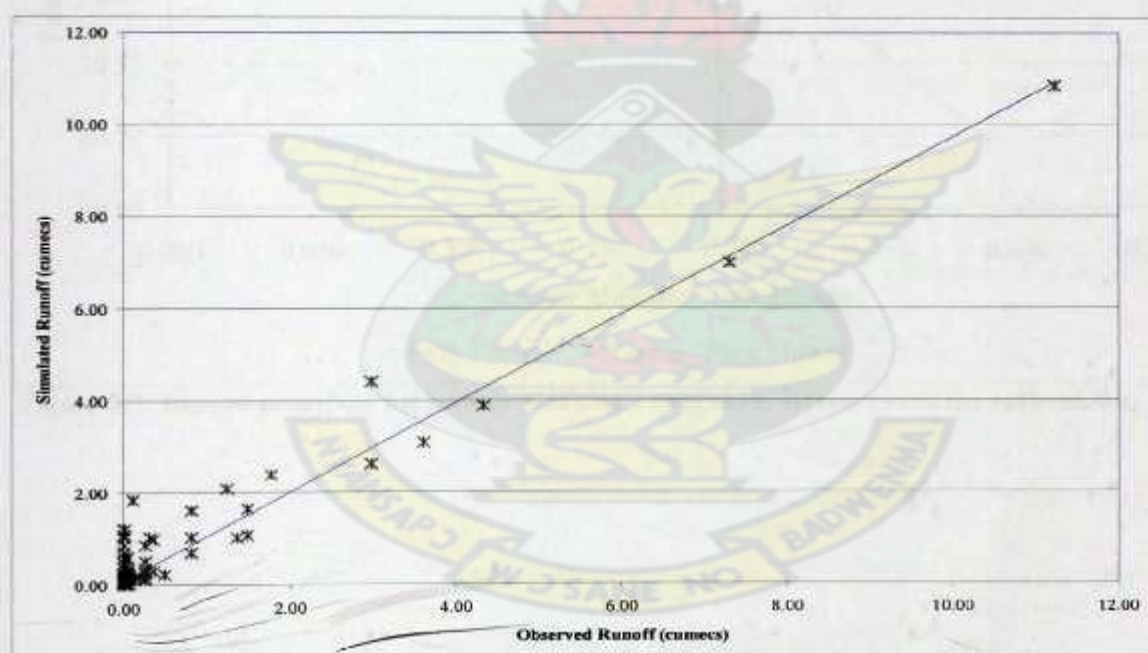

Figure 5-6: A plot of simulated flow against the observed flow (Coefficient of determination)

5.2.2.1 Model Sensitivity

The calibrated surface and channel Manning's roughness coefficients were increased one at a time by 10% from -50% to +50%. The corresponding peak flows were then plotted against the incremental Manning's roughness coefficients. Figure 5-7 and 5-8 presents the results of the simple sensitivity analysis. The two figures show a linear

66

relationship between the Manning's roughness coefficients with that of the peak

flows. The figures also show a decline of the peak flows as the Manning's roughness

coefficients increases indicating an inverse relation between the peak flows and the

coefficients. The red arrow shows the peak flows at the calibrated Manning's
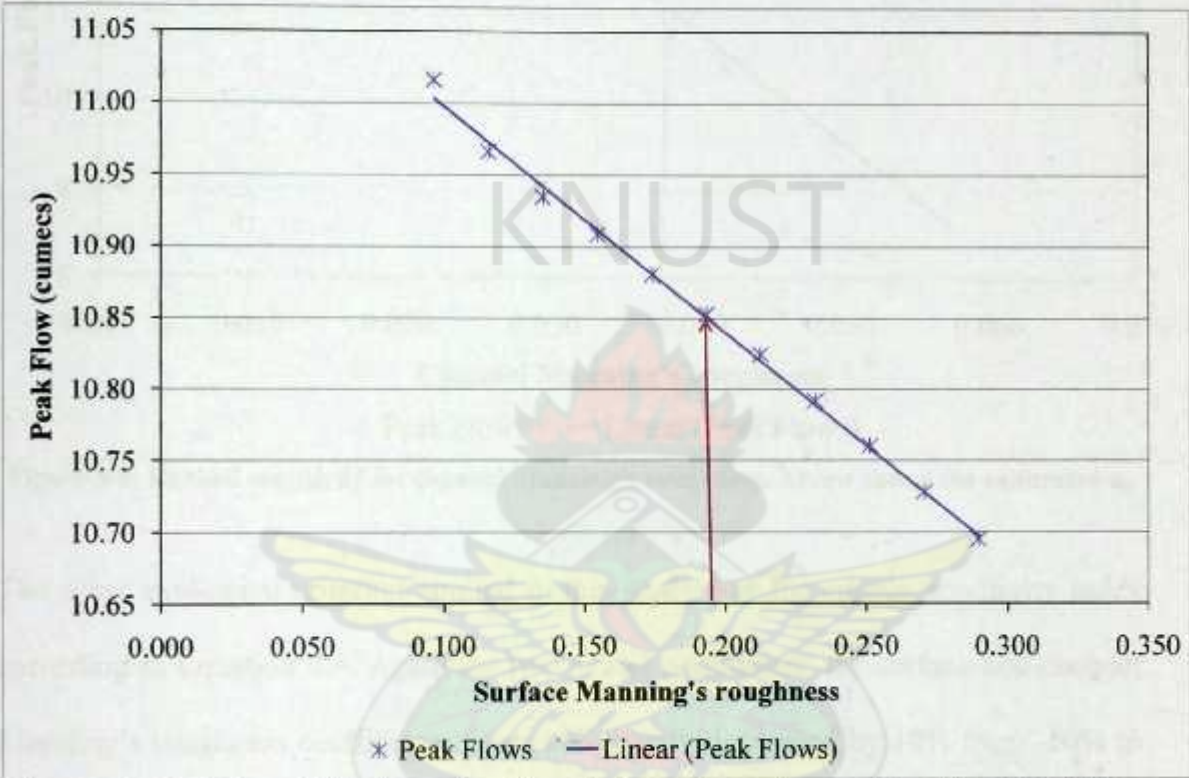
roughness coefficients.

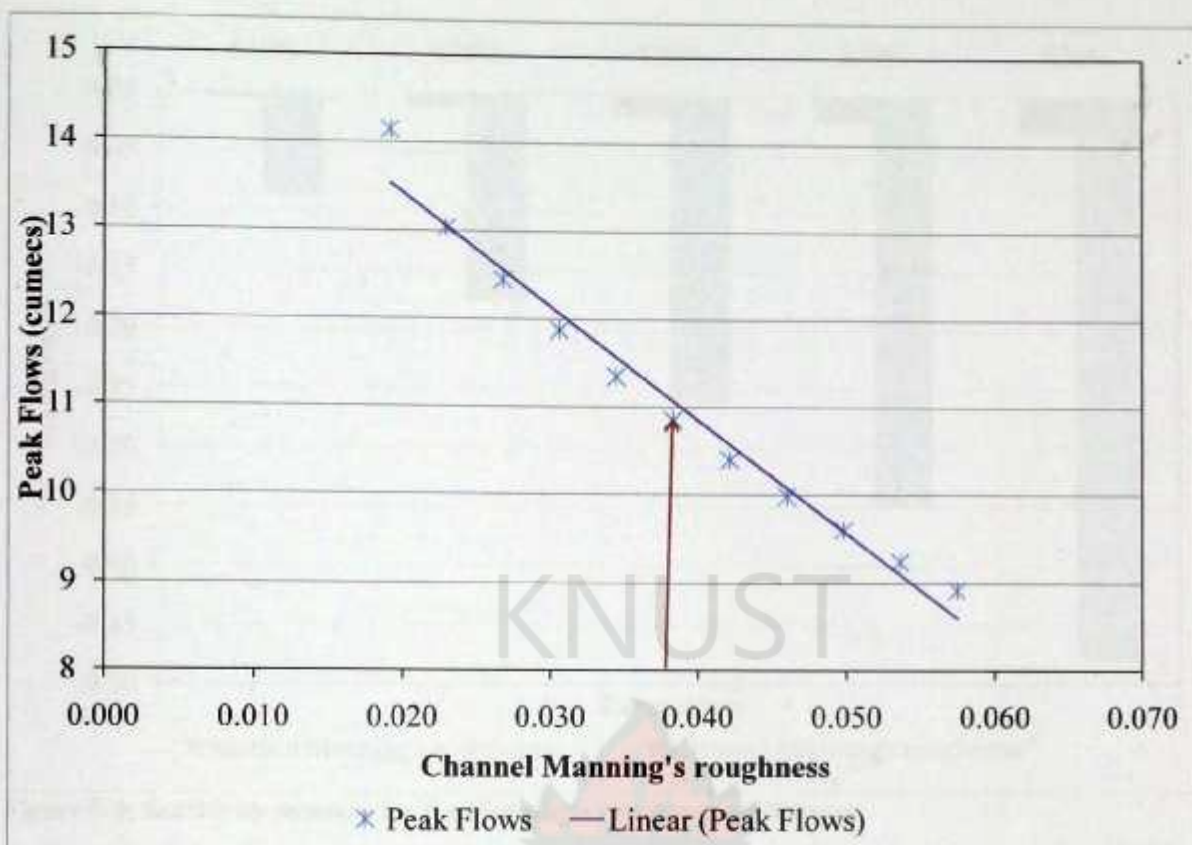**Figure 5-7: Ranked sensitivity for surface Manning's roughness. Arrow shows the calibrated n.**

Figure 5-8: Ranked sensitivity for channel Manning's roughness. Arrow shows the calibrated n_c

The other evaluation criterion applied in this study was the simple sensitivity index according to Equation 4.4. Again the two model parameters, the surface and channel Manning's roughness coefficients, were individually increased by 10% from -50% to +50% and the sensitivity index computed by Equation 4.4. A plot of sensitivity verses the parameter values is presented in Figure 5-9. The figure indicates that, the model output shows a significant sensitivity to variations in the channel Manning's roughness coefficient compared to that of the surface Manning roughness coefficient.
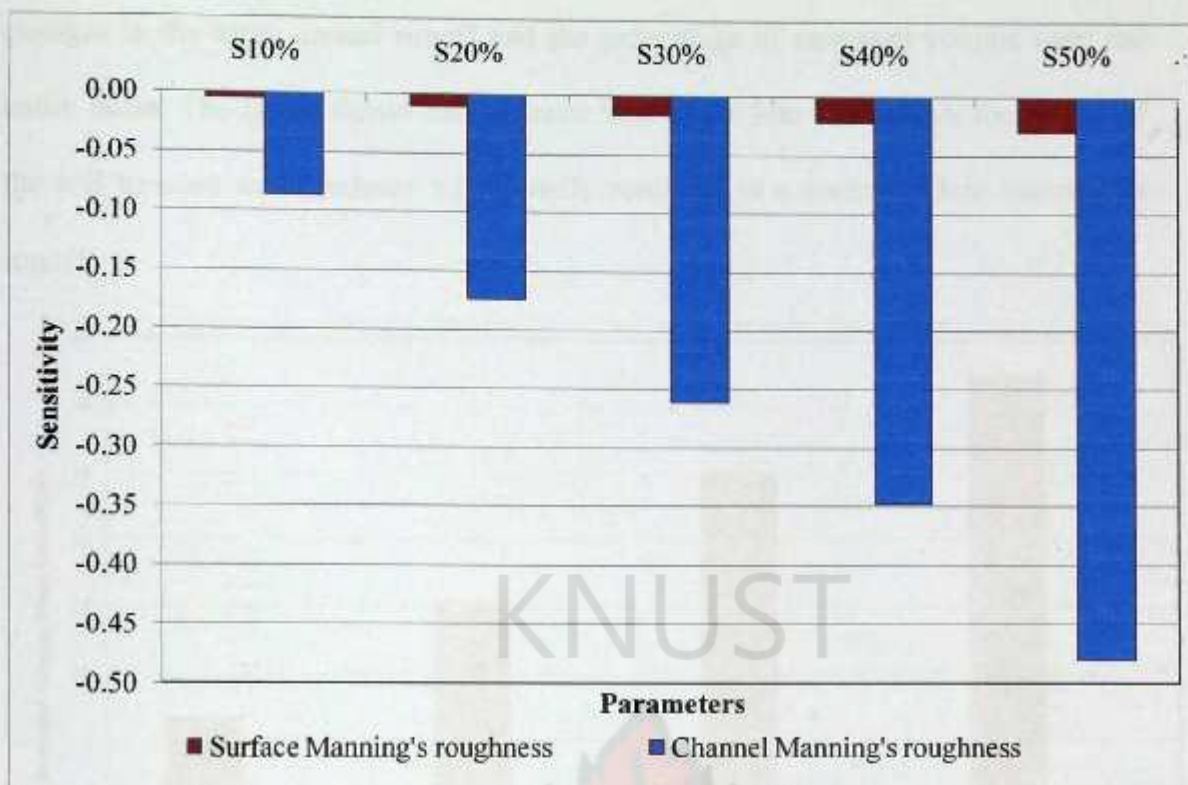
Figure 5-9: Sensitivity measure for the Manning's roughness coefficients

5.2.3 Model Application

5.2.3.1 Land-use Simulation Experiments

Following the satisfactory performance of the model in reproducing close to the measured runoff, the effects of proportional changes in land-use scenarios were simulated.

In the first scenario, an increase in cultivation of the uncultivated portions of the study site was simulated. In this scenario, the uncultivated portion of the land-use was randomly decrease by 20%, 40%, 60% and 80% and converted into cultivation. This resulted in an increase in the mean annual runoff over the calibrated mean annual runoff by 6.78%, 15.63%, 25.26% and 32.62% respectively. Figure 5-10 presents the general relationship between the proportionate land-use changes with respect to

changes in the mean annual runoff and the percentage of saturated volume over the entire basin. The figure shows that as more land is put into cultivation, the ability of the soil to store water reduces significantly resulting in a correspondent increase in runoff.
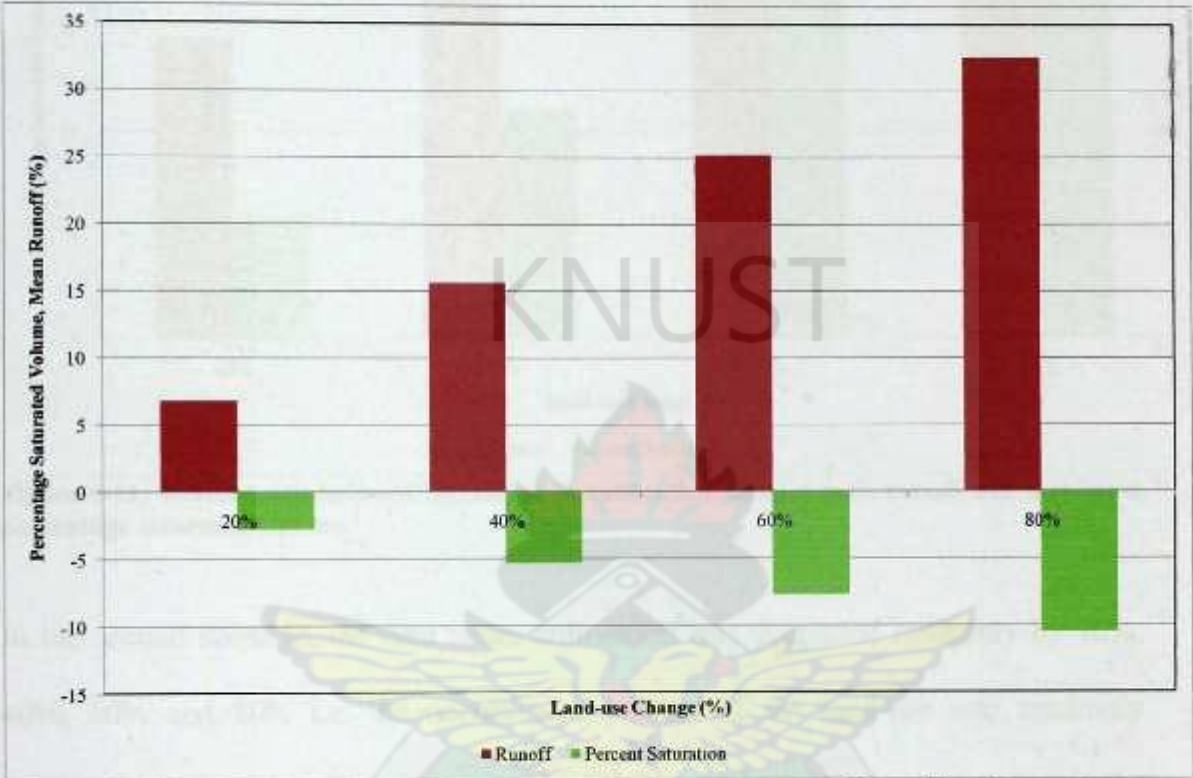

Figure 5-10: Relationship between increment in cultivation, mean annual runoff and percentage of saturated volume.

On the other hand, Figure 5-11 below illustrates the relationship between changes in land-use, peak annual runoff and percentage of saturated volume. As shown in the figure, increasing the area covered by tillage results in increasing annual peak runoff till a threshold of 40% change in land-use after which declining in annual runoff peaks are observed. However, unlike the peak runoffs, the maximum percentage saturated volume increased with increasing tillage area. The trend exhibited by the peak runoffs could be due to low catchment response as a result of the amount of water needed to saturate the soils after increment in the area that is put under cultivation.
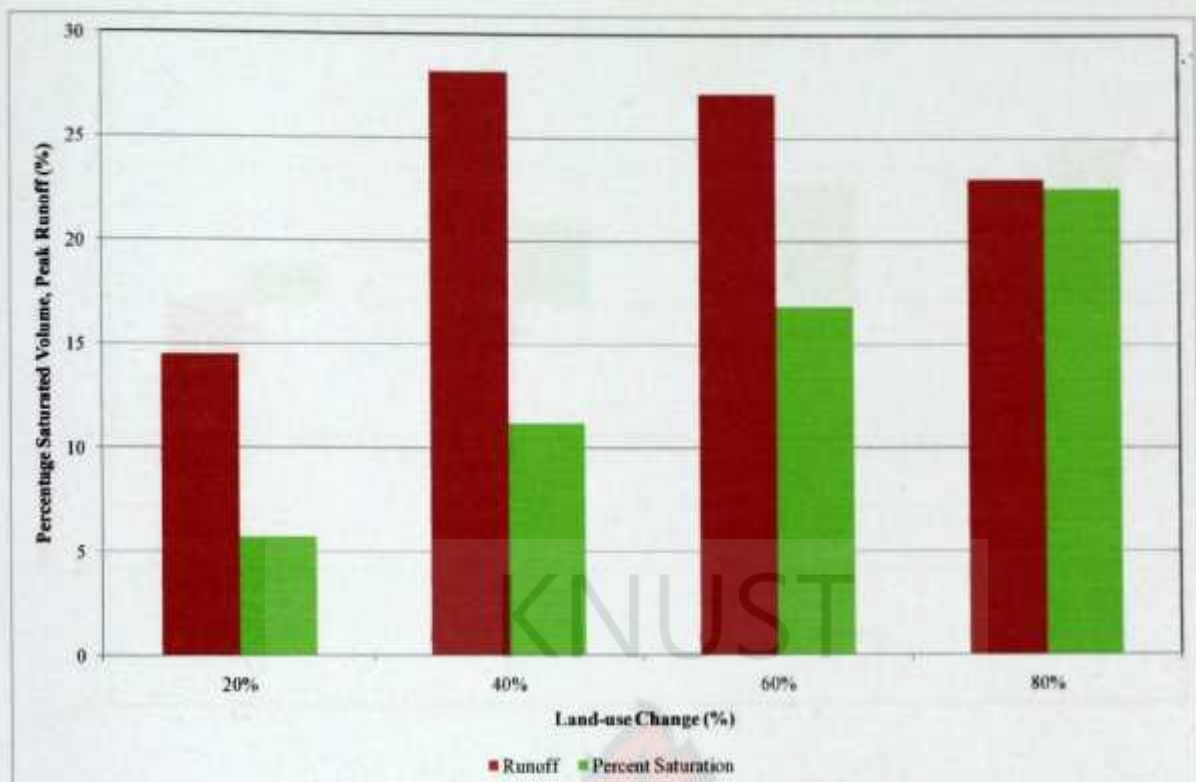
70

Figure 5-11: Relationship between increment in cultivation, annual peak runoff and maximum percentage saturated volume.

In the second scenario, the area under cultivation was decreased randomly by 20%, 40%, 60% and 80% i.e. the uncultivated portion of the land-use was randomly increased by practicing tillage conservation. This practice resulted in a decrease in the mean annual runoff over the calibrated mean annual runoff by 2.37%, 6.25%, 10.09% and 13.17% respectively. Figure 5-12 presents the general relationship between the proportionate land-use changes with respect to changes in the mean annual runoff and the percentage of saturated volume over the entire basin. The figure shows that as more land is conserved through no-till practices, the movement of water into the soils and subsequently the percentage saturated volume is increased significantly resulting in a correspondent decrease in runoff, Ward and Elliot (1995).
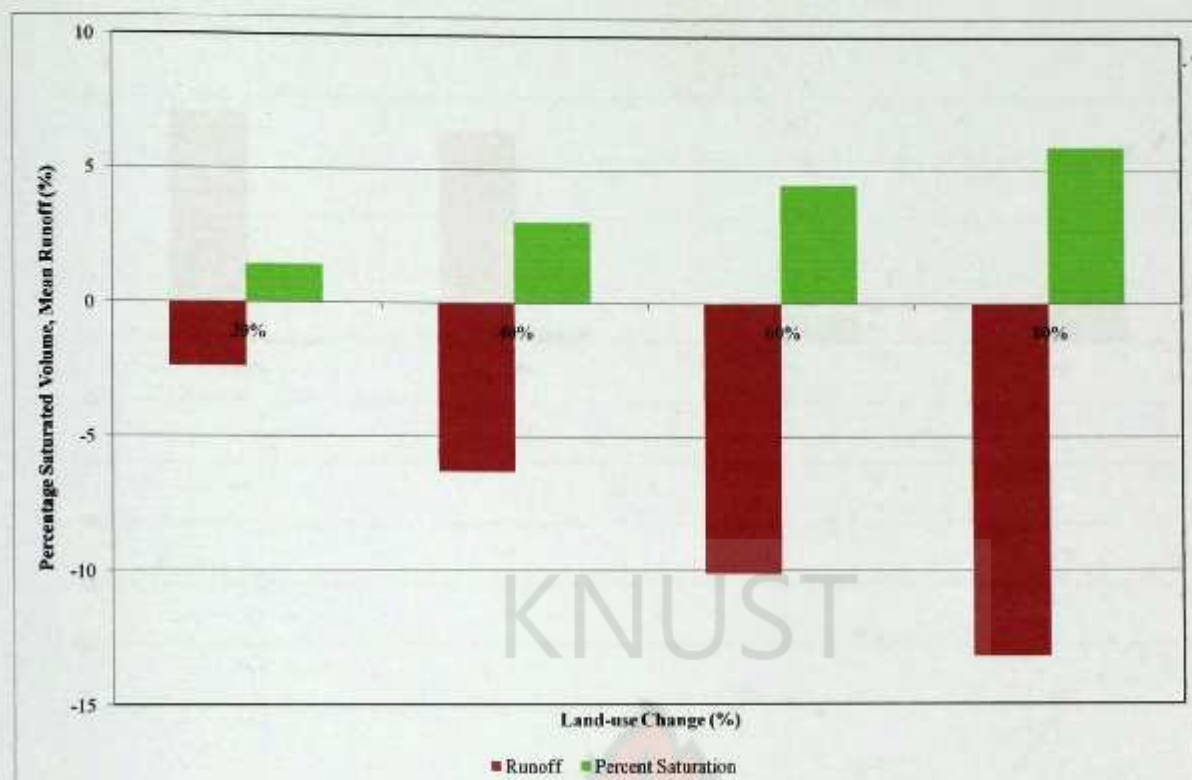
Figure 5-12: Relationship between increment in the uncultivated area, mean annual runoff and percentage of saturated volume.

With respect to the annual peak flows, Figure 5-13 below illustrates the relationship between changes in land-use i.e. tillage conservation, peak annual runoff and percentage of saturated volume. As shown in the figure, increasing the uncultivated area by 20% corresponds to an increase in the annual peak runoff but a reduction in the percentage saturated volume. However, further increases in tillage conservation results in decreasing annual peak runoffs with corresponding increases in the maximum percentage saturated volume.
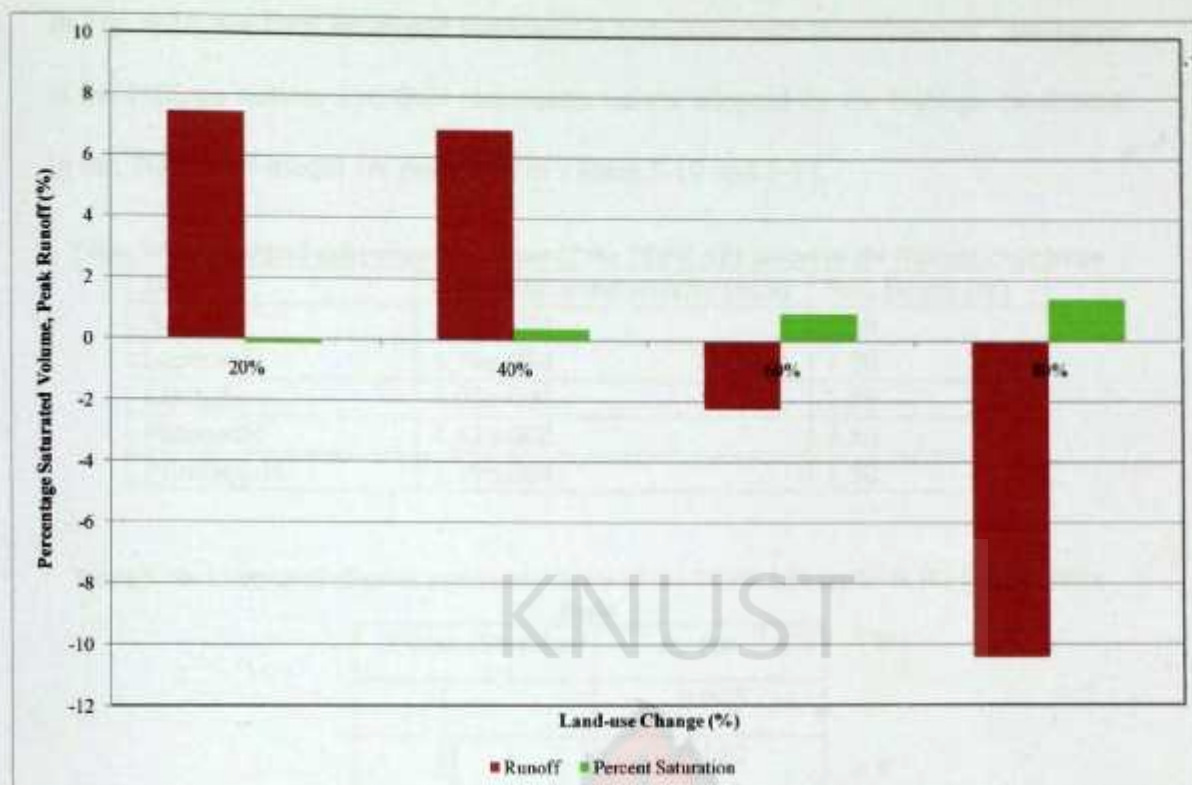
Figure 5-13: Relationship between increment in the uncultivated area, annual peak runoff and percentage of saturated volume.

5.2.3.2 Data Generation in the Nabogo catchment

The model was applied in the Nabogo gauging ststion, which is the outlet of the basin in this study, to generate runoff for possible in-filling of missing data in the basin. The application period, 1st March 2001 to 28th February 2005, was chosen because of the hydrological data consistency in that period, although there were still some missing data.

Having calibrated the model and verified its suitability in the experimental site, and having undertaken sensitivity analysis and noting that the model is very sensitive to the channel Manning's roughness coefficient, only the surface Manning's coefficient was calibrated in the Nabogo sub-catchment.

73

In Fig. 4-16, the final simulated discharge is compared with the "observed" discharge at the Nabogo station. The final parameters values adopted for the Nabogo catchment in the TOPKAPI model are presented in Tables 5-10 and 5-11.

Table 5-9: Calibrated soil parameter values of the TOPKAPI model in the Nabogo river basin

Soils	Hydraulic conductivity (m/s)	Soil Depth (m)
Acrisols	9.17e-004	1.50
Leptosols	1.74e-004	1.50
Lixisols	6.03e-004	1.50
Planosols	4.42e-006	1.50
Plinthosols	1.39e-004	1.50

Table 5-10: Calibrated channel parameter values of the TOPKAPI model in the Nabogo river basin

Order (Strahler)	n_c $(m^{-1/3} s^{-1})$
I	0.045
II	0.040
III	0.035
IV	0.030
V	0.030

It is clearly seen from Figure 5-10 that the model performance has given a satisfied result, especially for the peak flows. With these calibrated model parameters, the TOPKAPI model can be used as a tool for filling-in gaps in the data set of the Nabogo river basin.
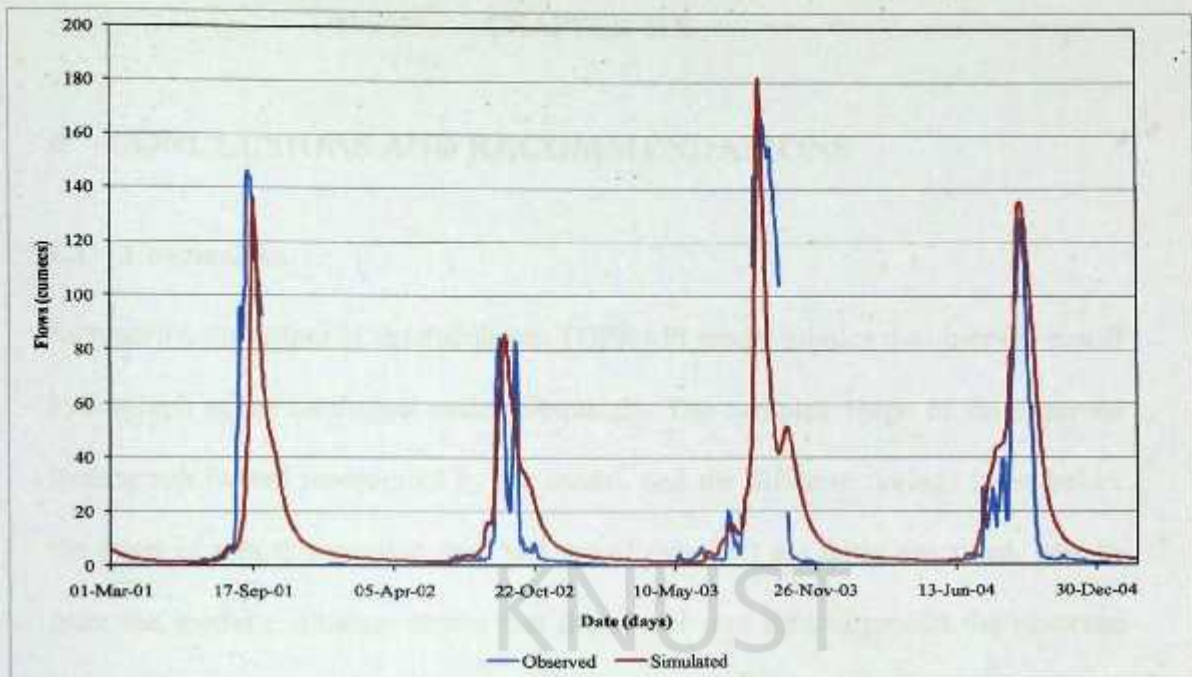
74

Figure 5-14: Comparison of observed and simulated runoff at Nabogo

6 CONCLUSIONS AND RECOMMENDATIONS

6.1 Conclusions

Summarily, the output of the distributed TOPKAPI model mimics the observed runoff hydrograph at the catchment outlet adequately. The complex shape of the observed hydrograph is well represented by the model, and the different timings (time before the onset of runoff; recession time and runoff duration) are fairly described. Results from the model evaluation shows that the model was able to predict the observed hydrograph with a coefficient of efficiency of 87.7%. The model was however unable to adequately account for the low flows in the catchment.

Results from the sensitivity analysis shows that the channel Manning's roughness coefficient has a higher effect on runoff generation than that of the surface Manning's roughness coefficient. It was also observed that the peak flows decreases with increasing Manning's roughness coefficients. Nonetheless, care must be taken when calibrating the channel Manning's coefficient since it is highly sensitivity to any form of variation.

Analyses were made to quantitatively assess the impact of land-use change on the watershed hydrology. Results from the first land-use scenario demonstrates that putting more land under cultivation results in declining water holding capacity of the soils with attendant increases in mean annual runoff.

The results from the second land-use scenarios also show that tillage conservation increases the soil water content with high percentage saturated volume. However, it

was also observed that decreasing the area under cultivation in the experimental site results in decreasing mean annual runoffs.

Results obtained from the model application at Nabogo, a sub-catchment of the Volta basin was also very encouraging. This presents an excellent tool for generating runoff data to fill-in gaps in the hydrological stations in the Volta basin.

6.2 Recommendations

In light of the results from both the field observations and the modeling techniques used in this study, the following recommendations in terms of field experimentation and possible applications and further extension of the model are proposed:

- Sustained long term studies on surface runoff process in the basin.
- Since the model was unable to adequately account for low flows in the basin, it would be challenging to attempt to couple the model with groundwater models such as MODFLOW to deal with the percolation aspects of the rainfall-runoff process.
- Given the sensitivity of hydrologic response to climatic conditions, future research should focus more attention on the use of climate scenarios to characterize hydrologic response for a range of climatic conditions. With a suitable weather generator it may be possible to predict hydrologic response from land-use and climate change for a range of climatic conditions.
- The Hydrological Services Department could also adopt and use the model to generate stream flows to fill-in missing data in the hydrological monitoring stations in the Volta basin.

77

Finally, further experiments should be carried out using the TOPKAPI in the middle and southern sectors of the Volta basin taking advantage of increasingly availability of topographic, land-use and soil maps at higher resolutions.

78

Reference

Abbott, M. B., Barthurst J. C, Cunge, J. A., O'Connell, P. E. and Rasmussen, J. (1986). An introduction to the European Hydrologie System—Système Hydrologique Européen "SHE" 1: history and philosophy of a physically based, distributed modelling system. J. Hydrol. 87,45-59.

Abbott, M. B., Barthurst J. C, Cunge, J. A., O'Connell, P. E. and Rasmussen, J. (1986). An introduction to the European Hydrologie System—Système Hydrologique Européen "SHE" 2: structure of a physically based, distributed modelling system. J. Hydrol. 87, 61-77.

Ajayi, A. E., Vlek, P. L. G., Denich, M., Martius, C., van de Giesen, N., (2004). Surface runoff and infiltration processes in the Volta Basin, West Africa: Observation and modeling. Ecology and Development Series No. 18, 2004. p2.

Andreini M., van de Geisen, N., van Edig, A., Fosu, M. and W. Andah, (2000). Volta Basin Water Balance. ZEF Discussion Papers on Development and Policy No. 21.

Bedient, P. B. and W. C. Huber. (1992). Hydrology and floodplain analysis. (2nd ed.). Addison-Wesley Publishing Company. p88.

Beven K. J. (1989). Changing ideas in hydrology - The case of physically-based models. J. Hydrol. 105: 157-172.

Beven K. J. and O'Connell P. E. (1982). On the role of distributed models in hydrology. Institute of Hydrology report 81, Wallingford, UK.

Beven K. J., Kirkby M. J. (1979). A physically based, variable contributing area model of basin hydrology. Hydrol. Sci. Bull., 24(1), 43-69.

79

Beven K., Lamb R., Quinn P., Romanowicz R., Freer J. (1995). TOPMODEL. In Computer Models of Watershed Hydrology, Singh V. P. (ed). Water Resources Publications: 627-668.

Binka, F. N., Ngom, P., Phillips, J. F., Adazu, K. F., and Macleod, B., (1999). Assessing Population Dynamics in a Rural African Society; Findings from the Navrongo Demographic Surveillance System. Journal of Biosocial Science 31, 375-391.

Chevallier P. and Planchon O. (1993). Hydrological process in a small humid savannah basin (Ivory Coast). J. Hydro.151: 173-191.

Dingman, S. L., (1994). Physical Hydrology. Macmillan Publishing Company, New York. p405.

Diskin, M. H. and Simon, E., (1979). The relationship between the time base of simulation models and their structure. Water Resources Bulletin, Vol. 15, No. 6 pp. 1716-1732.

Dooge, J. C. I., (1973). Linear theory of hydrologic systems. Technical Bull. No. 1468, USDA, ARS, Washington, DC, p327.

FAO (1995), World Agriculture: Towards 2010, An FAO Study. N. Alexandratos (Editor) FAO, Rome. pp 210.

Franchini M., Wendling J., Obled C., and Todini E. (1996). Physical interpretation and sensitivity analysis of the TOPMODEL. J. Hydrol. 175: 293-338.

Gaume, E., Villeneuve, J.-P. & Desbordes, M., (1998). Uncertainty assessment and analysis of the calibrated parameter values of an urban storm water quality model, J. Hydrol. 210, 38-50.

Harlin, J. and Kung, C. S., (1992). Parameter uncertainty and simulation of design floods in Sweden. J. Hydrol. 137, 209-230.

Hobo BoxCar Pro 4.3, (2002). User Guide, Onset Computer Corporation, Bourne MA 02532, USA.

Jakeman, A. J. & Homberger, G. M., (1993). How much complexity is warranted in a rainfall-runoff model. Wat. Resour. Res 29(8), 2637-2649.

Johnstone, D., and Cross W. P., (1949). Elements of Applied Hydrology, Ronald Press Company, New York.

Klute, A. and Dirksen C., (1986). Hydraulic conductivity and diffusivity: Laboratory methods. In: Klute A (ed) Methods of Soil Analysis, Part 1, 687-734. Madison, WI: Am. Soc. Agron.

Kuichling, E. (1989). The relation between the rainfall and the discharge of sewers in populous districts. ASCE Trans., vol. 20, p1-56.

Landon, J. R., (1991). A booker tropical soil manual: A handbook for soil survey and agricultural land evaluation in the tropics and subtropics. Booker Tate, Thame, Oxon, UK, 58-125.

Linsley, R. K., Kohler M. A. and Paulhus J. L. H., (1949). Applied Hydrology. McGraw-Hill Co., New York, p689.

Lloyd-Davies, D. E. (1906). The elimination of storm water from sewage systems. Inst. Civ. Eng. Proc., vol. 164, 41-67.

Mein, R. G. & Brown, B. M. (1978). Sensitivity of optimized parameters in watershed models. Wat. Resour. Res. 14(2), 299-303.

Melching, C. S., Yen, B. C. & Wenzel, H. G. Jr (1990). A reliability estimation in modeling watershed runoff with uncertainties. Wat. Resour. Res. 26(10), 2275-2286.

Moore I. D, Grayson, R. B. and Ladson A. R. (1991) Digital terrain modeling: A review of hydrological, geomorphological and biological applications. Hydrol. Processes 5:3-30.

Mroczkowski, M., Raper, G. P. and Kuczera, G., (1997). The quest for more powerful validation of conceptual catchment models. Wat. Resour.Res. 33(10), 2325-2335.

Mulvaney, T. J., (1851). On the use of self-registering rain and flood gauges. Inst. Civ. Eng. (Ireland) Trans., vol. 4(2), p1-8.

Nash, J. E. and Sutcliffe, J. V., (1970). River flow forecasting through conceptual models, 1, a discussion of principles. J. Hydrol. 10 (1): 282–290.

Opoku-Ankomah, Y., (2000). Impacts of Potential Climate Change on River Discharge in Climate Change Vulnerability and Adaptation Assessment on Water Resources of Ghana. Water Research Institute (CSIR), Accra. Ghana.

Rawls, W. J, Brakensiek, D. L., and Saxton, K. E. (1982). Estimation of soil water properties. Transactions of ASAE 25: 1316-1320.

Rosenblueth, A. and Wiener, N., (1945). Role of models in science. Phil Sci. 7(4): 316-321.

Shaake, J. C., Geyer, J. C., and Knapp, J. W. (1967). Experimental examination of the rational method. J. Hydrol. Div., ASCE 93(6):353-370.

Sherman, L. K., (1932). Stream flow from rainfall by unit graph method, Eng. News Record 108:501-505.

Singh, V. P., (1995). Computer models of watershed hydrology. Water Resources Publications, p1.

Sivapalan, M., Beven, K. J., Wood, E. F., (1987). On hydrological similarity 2. A scaled model of storm runoff production. Water Resour. Res., 23(12): 2266-2278.

Smith, R. E. and Hebbert, R. H. B., (1983). Mathematical simulation of interdependent surface and subsurface hydrological processes, Water Resour. Res., 19(4), 987–1001.

Taylor, C. S., (1952). The vegetation zones of the Gold Coast. Govt. Printer. Forestry Department Bulletin No.4, Accra.

The VAHMPIRE Project, http://paleo.ija.csic.es/rn/hidro/objectiv.html

Thornthwaite, C. W. and J. R. Mather, (1955). The Water Balance. Publications in Climatology, Vol. 8, No. 1, Drexel Institute of Technology, Laboratory of Climatory, Centerton, N. J.

Todini E.. (1995). New trends in modelling soil processes from hillslope to GCM scales. In The Role of Water and the Hydrological Cycle in Global Change, Oliver H.R. and Oliver S.A. (eds). NATO ASI Series, Series I: Global Environmental Change, 31: 317-347.

Todini E.. (1996). The ARNO rainfall-runoff model. J. Hydrol., 175: 339-382.

Todini, E. (1988). Rainfall-runoff modeling past, present and future. J. Hydrol. 100, 341-352.

Todini, E. and Dümenill L., (1999). Estimating large-scale runoff. Global Energy and Water Cycles. Browning K.A. & Gurney R.J. (eds). Cambridge University Press: 265-281.

Todini, E., (1995). New trends in modeling soil processes from hillslope to GCM scales. In The Role of Water and the Hydrological Cycle in Global Change,

Oliver H.R. and Oliver S.A. (eds). NATO ASI Series, Series I: Global Environmental Change, 31: 317-347.

Troch P.A., Smith J.A., Wood E.F. and de Troch F.P. (1994). Hydrologic controls of large floods in a small basin: central Appalachian case study. J. Hydrology 156 (1-4) pp. 285-309.

van de Giesen, N.C., Stomph T. J. and de Ridder N. (2000). Scale effects of Hortonian overland flow and rainfall-runoff dynamics in a West African catena landscape. Hydrological Processes 14 (1): 165-175.

van der Perk. M. and Bierkens, M. F. P. (1997). The identifiability of parameters in a water quality model of the Biebrza River, Poland. J. Hydrol. 200, 307-322.

Vivoni, E. R., Entekhabi, D. and Ivanov, V. Y., (2007). Controls on runoff generation and scale-dependence in a distributed hydrologic model, Hydrol. Earth Syst. Sci. Discuss., 4, 983-1029.

Ward, A. D. and Elliot, W. J., (eds). (1995). Environmental Hydrology. Lewis Publishers. p12.

Ward, A. D. and Elliot, W. J., (eds). (1995). Environmental Hydrology. Lewis Publishers. p62-69.

Warrick A W and Nielson DR (1980). Spatial variability of soil physical properties in the field. In: Hillel D (ed) Applications of soil physics, Academic press, New York, p319-344.

Wilson, J. P., and Gallant, J. C., (2000). Digital Terrain Analysis. In: Wilson JP and Gallant JC (eds) Terrain Analysis: Principles and Application, John Wiley and Sons, New York, p1-27.

WMO-WHYCOS, (2005). Hydrological information systems for integrated water resources management - WHYCOS Guidelines. WMO/TD-No.1282, p 5-12.

Zhao, R .J., (1977). Flood forecasting method for humid regions of China. East China College of Hydraulic Engineering, Nanjing.

Zhiyu, Liu, (2002). Toward A Comprehensive Distributed/Lumped Rainfall-Runoff Model, University of Bologna.